DEVELOPMENT, IMPLEMENTATION, AND TESTING OF A TIGHTLY COUPLED INTEGRATED INS/GPS SYSTEM

A THESIS SUBMITTED TO
THE GRADUATE SCHOOL OF NATURAL AND APPLIED SCIENCES
OF
THE MIDDLE EAST TECHNICAL UNIVERSITY

BY

ALPER ÖZTÜRK

IN PARTIAL FULFILLMENT OF THE REQUIREMENTS FOR THE
DEGREE OF MASTER OF THESIS
IN
THE DEPARTMENT OF ELECTRICAL AND ELECTRONICS
ENGINEERING

AUGUST 2003

Approval of the Graduate School of Natural and Applied Sciences

Prof. Dr. Canan Özgen
Director

I certify that this thesis satisfies all the requirements as a thesis for the degree of Master of Science.

Prof. Dr. Mübeccel Demirekler
Head of Department

This is to certify that we have read this thesis and that in our opinion it is fully adequate, in scope and quality, as a thesis for the degree of Master of Science.

Prof. Dr. Mübeccel Demirekler
Supervisor

Examining Committee Members

Prof. Dr. Kemal Leblebicioğlu (Chairman)

Prof. Dr. Mübeccel Demirekler

Prof. Dr. İsmet Erkmen

Assoc. Prof. Dr. Tolga Çiloğlu

Dr. Ayşe Pınar Koyaz

ABSTRACT

DEVELOPMENT, IMPLEMENTATION, AND TESTING OF A TIGHTLY COUPLED INTEGRATED INS/GPS SYSTEM

Öztürk, Alper

M.S., Department of Electrical and Electronics Engineering

Supervisor: Mübeccel Demirekler

August 2003, 90 Pages

This thesis describes the theoretical and practical stages through development to testing of an integrated navigation system, specifically composed of an Inertial Navigation System (INS), and Global Positioning System (GPS). Integrated navigation systems combine the best features of independent systems to bring out increased performance, improved reliability and system integrity. In an integrated INS/GPS system, INS output is used to calculate current navigation states; GPS output is used to supply external measurements, and a Kalman filter is used to provide the most probable corrections to the state estimate using both data.

Among various INS/GPS integration strategies, our aim is to construct a tightly coupled integrated INS/GPS system. For this purpose, mathematical models of INS and GPS systems are derived and they are linearized to form system dynamics and system measurement models respectively. A Kalman filter is designed and implemented depending upon these models. Besides these, based on the given aided navigation system representation a quantitative measure for observability is defined using Gramians. Finally, the performance of the developed system is evaluated with real data recorded by the sensors. A comparison with a reference system and also with a loosely coupled system is done to show the superiority of the tightly coupled structure. Scenarios simulating various GPS data outages proved that the tightly coupled system outperformed the loosely coupled system from the aspects of accuracy, reliability and level of observability.

Keywords: Inertial Navigation System (INS), Global Positioning System (GPS), Integrated Navigation, Tightly Coupled, Loosely Coupled, Observability.

ÖZ

SIKICA BAĞLI BÜTÜNLEŞTİRİLMİŞ INS/GPS SİSTEMİNİN GELİŞTİRİLMESİ, GERÇEKLEŞTİRİLMESİ VE TEST EDİLMESİ

Öztürk, Alper

Yüksek Lisans, Elektrik ve Elektronik Mühendisliği Bölümü

Tez Yöneticisi: Mübeccel Demirekler

Ağustos 2003, 90 Sayfa

Bu tez çalışmasında, özgül olarak bir Ataletsel Seyir Sistemi (INS) ve Küresel Konumlama Sistemi'nden (GPS) meydana gelen, bütünleştirilmiş bir seyir sisteminin, geliştirilmesinden test edilmesine kadar olan teorik ve pratik aşamaları anlatılmıştır. Bütünleştirilmiş seyir sistemleri, bağımsız sistemlerin en iyi özelliklerini birleştirerek iyileştirilmiş performans, geliştirilmiş güvenilirlik ve sistem bütünlüğü ortaya çıkarır. Bütünleştirilmiş bir INS/GPS sisteminde, INS çıktıları güncel sistem durum değişkenlerini hesaplamak için; GPS çıktıları harici ölçümleri oluşturmak için ve Kalman filtre de bu iki bilgiyi kullanarak durum değişkenlerine en olası düzeltmeleri sağlamak için kullanılır.

Amacımız, varolan çeşitli INS/GPS bütünleştirme stratejileri arasından, sıkıca bağlı bütünleştirilmiş bir INS/GPS sistemi oluşturmaktır. Bu amaçla, sırasıyla sistem dinamiği ve sistem ölçüm modelini oluşturabilmek için, INS ve GPS sistemlerinin matematiksel modelleri çıkarılmış ve doğrusallaştırılmıştır. Bu modellere dayanan bir Kalman filtre tasarlanmış ve gerçekleştirilmiştir. Bunların yanı sıra, verilmiş olan destekli seyir sistemi gösterimine dayanan, gözlemlenebilirlik için nicel ölçütler, Gramian'lar kullanılarak tanımlanmıştır. Son olarak, algılayıcılar tarafından kaydedilen gerçek veriler kullanılarak sistemin değerlendirilmesi yapılmıştır. Referans bir sistemle karşılaştırmanın yanı sıra, sıkıca bağlı yapının üstünlüğünün gösterilmesi için gevşek bağlı bir sistemle de karşılaştırmalar yapılmıştır. GPS bilgi kesintilerini simüle eden çeşitli senaryolar, hassasiyet, güvenilebilirlik ve gözlemlenebilirlik seviyesi açılarından sıkıca bağlı sistemin, gevşek bağlı sistemin çok üstünde bir performansa ulaştığını göstermiştir.

Anahtar Kelimeler: Ataletsel Seyir Sistemi (INS), Küresel Konumlama Sistemi (GPS), Bütünleştirilmiş Seyir, Sıkıca Bağlı, Gevşek Bağlı, Gözlemlenebilirlik.

ACKNOWLEDGEMENTS

I would like to express my sincere appreciation to my supervisor Prof. Dr. Mübeccel Demirekler for her continued guidance, also patience and support throughout my research. She provided advice, and assistance that greatly enhanced my studies and experience.

Thanks go to my manager Dr. Murat Eren for his patience and support from beginning to end of my M.Sc. program. I am also grateful to several of my colleagues, especially those who shared my office and thereby my problems. These include Naci Orhan, Celal Ademoğlu, and Salim Sırtkaya. Volkan Nalbantoğlu also spent several hours talking me through concepts that were once foreign to me.

ASELSAN A.Ş. who supported this work is greatly acknowledged.

And last, but certainly not least, I offer sincere thank for my friends and my family. My girlfriend, Zeynep, always supported and believed in me. My family put up with being second during this thesis and they did not give up their continuous love and understanding.

TABLE OF CONTENTS

LIST OF TABLES

TABLE

LIST OF FIGURES

FIGURE

CHAPTER 1

INTRODUCTION

1.1 Background

Navigation is a very ancient skill or art which has become a complex science due to the developments in technology and increasing complexity of vehicle systems. This progress increased the need to be able to determine the position, velocity and orientation of a vehicle with a greater demand on accuracy. Higher accuracy demand, directed people to develop higher cost sensors and this as a result, revealed the concept of integrated navigation which makes use of lower cost systems to produce higher accuracy ones.

The Global Positioning System (GPS) has been proven to be an accurate positioning sensor for a variety of applications (Daljit and Grewal, (1995)) and has made land navigation applications affordable and dependable. The quality of GPS position estimates is basically time-invariant and independent of location and weather. A drawback of GPS in general, is the requirement to maintain line of sight visibility to the satellites being tracked. Under signal masking conditions, the number of visible satellites can be significantly reduced, leading to a loss of navigation solution or decreasing strength in the estimation process and lower position accuracies. As a summary, these effects cause short term data gaps and high frequency faults in the GPS navigation output.

Unlike GPS, Inertial Measurement Units (IMUs) are completely autonomous (self-contained) instruments that sense accelerations and rotation rates in three orthogonal axes. An Inertial Navigation System (INS), which contains an IMU as one of its components, integrates the rotation rates to obtain orientation changes, and doubly integrates the accelerations to obtain velocity and position increments (Jekeli, 2000). Despite the advantage of self-containment, sensor inaccuracies such as gyro drifts and accelerometer biases cause a rapid degradation in inertial position quality. Higher quality inertial sensors provide higher accuracies for longer times but this brings even higher costs. So in general, measurements independent of the inertial equipment are incorporated into the navigation computations to improve accuracy. Among the several types of external measurements that can be employed, our emphasis is on the use of GPS information.

The complementary characteristics of INS, self-containment and high accuracy in short-term navigation; and GPS, invariable characteristics over time and having bounded errors, is the reason for these two systems to be widely used as integrated navigation systems. The advantages of GPS/INS integrated systems, relative to “GPS-only” or “INS-only”, are reported to be a full position, velocity and attitude solution, improved accuracy and availability, smoother trajectories, greater integrity and reduced susceptibility to jamming and interference, as discussed in Hartman (1988) and Greenspan (1996).

Kalman filtering exploits a powerful synergism between GPS and INS. Kalman filter is able to take advantage of these complementary characteristics to provide a common, integrated navigation implementation with performance superior to that of either subsystem. By using statistical information about the errors in both systems, it is able to combine a system with tens of meters position uncertainty with another system whose position uncertainty degrades at kilometers per hour and achieve bounded position uncertainties in the order of meters (Grewal and Weill (2001)).

The level of integration used in a GPS/INS system can vary from application to application. Typically, three main levels of integration are defined, namely loosely coupled integration, tightly coupled integration and ultra-tight (or deep) integration. The latter approach is typically performed at the hardware level and has therefore been implemented by equipment manufacturers only. The other two strategies are used in approximately equal quantities in the literature, although recently the tight integration seems to be gaining popularity. Each approach has its own advantages and disadvantages, but there has been little comparison between the two.

1.2 Objectives

This thesis addresses the issue of development, implementation, and testing of a tightly coupled integrated INS/GPS system which is intended to be used for land vehicles, pointing out mainly the positioning aspects.

Development stage comprises understanding the working principles of the individual systems in detail; deriving the well known equations for these systems and adopting those equations for our specific case; designing a Kalman filter to optimally integrate both systems; and analyzing the observability concepts. Implementation stage is composed of building up hardware and software setups to use sensors in hand, recording real data from these sensors, and writing algorithms to produce results. Test stage includes fine-tuning the system by trial and error method; preparing the necessary documentation and plots; comparing the results of developed system with a reference system and as well as with a loosely coupled system.

The objectives of this study are to investigate the following parameters of the integration of an INS with GPS:

- *Integrated System's Reliability.* By assessing the ability of a system to reject erroneous observations, the overall robustness of the system can be assessed. Comparing scenarios which use GPS-only or INS-only and GPS/INS systems will provide valuable insight into the benefit of using the integrated system.

- *System Positioning Accuracy During GPS Data Outages.* Under operational conditions, GPS data outages occur with varying durations. The duration for which the integrated system can navigate through such data outages with satisfactory accuracy will determine the potential uses of the system. Data outages can vary in severity from complete data outages where no satellite signals are available, to partial data outages where sub-optimal or insufficient satellite visibility is available.

Simulation of complete and partial GPS data outages of varying duration is used to assess the performance of the integrated system.

- *Observability of Aided Navigation System.* The concept of observability has a considerable effect in success of an integrated system. Although intuitive approaches are met in the literature, quantitative analyses are not done for specifically the tightly coupled integrated navigation system. The observability analysis carried out in this study will investigate these intuitive concepts by a quantitative approach.

- *Impact of Integration Strategy On Overall System Performance.* While loosely and tightly coupled integrations are common in practice, the benefits of each approach in operational conditions are not well demonstrated. Consequently, each of the above parameters will be investigated using a loosely and tightly coupled integration strategy.

1.3 Thesis Outline

Chapter 2 provides the necessary background into navigation systems, specifically the Global Positioning System and the Inertial Navigation System. Equations governing the calculation of navigation states are derived for these systems. These equations are linearized to form the system error dynamic model and system measurement model. Finally using these models, a Kalman filter is designed to integrate INS and GPS outputs.

Chapter 3 provides the background into the concept of observability, observability Gramian and observability measure. Using these concepts, a representation of the aided INS system is constituted. The observability of the tightly coupled system is mentioned. Finally, the computation method of the observability measure used in this study is given.

Chapter 4 provides results for the navigation system developed. Findings of observability analysis, comparisons of tightly coupled integrated navigation system with a reference system and with a loosely coupled system are given in the direction of objectives listed in the previous section.

Chapter 5 provides the summary for the overall study.

CHAPTER 2

NAVIGATION SYSTEMS

2.1 Introduction

This chapter provides the necessary background information on navigation systems, specifically the “Global Positioning System (GPS)” and “Inertial Navigation System (INS)”. Furthermore, the chapter will provide, as a contribution, the inertial navigation and GPS equations and models needed for the integration of both systems. These equations will be linearized to develop error equations. Then, “Kalman Filter” algorithm and equations used to fuse GPS and INS measurements will be discussed. Finally, the overall navigation Kalman filter structure that is developed based on the GPS and INS models will be provided. This structure forms the basis of efforts for the implementation of the Kalman filter.

2.2 Global Positioning System

Global Positioning System (GPS) is a space-based radio navigation system. The system is developed and currently operated by the Navstar GPS Joint Program Office (JPO). GPS provides accurate position, velocity and time (PVT) information to an unlimited number of users. This information is available all around the world regardless of the weather conditions. GPS consists of three major system segments for operation: Space, Control and User.

2.2.1 System Operation

The Space Segment consists of GPS satellites. The current constellation of the GPS system includes 31 satellites. 24 of these satellites are enough for nominal full operation. GPS satellites orbit around the earth in a path of 11 hour and 58 minutes and have an average orbit altitude of 20200 kilometers. They are oriented such that a user on the surface of the earth sees at least 4 of them simultaneously. Each satellite in the constellation broadcasts RF signals that are carrying information. This information includes a coded Navigation Data and a code signal used for ranging purposes.

The Control Segment consists of a network of monitoring and control facilities which are used to manage the satellite constellation and update the satellite navigation data messages. The control of satellite station-keeping maneuvers, re-configuration of redundant satellite equipment, regularly updating the navigation messages transmitted by the satellites, and various other satellite health monitoring and maintenance activities are the major missions of the Control Segment. The monitor stations passively track all GPS satellites in view, collecting ranging data from each satellite. The Control Segment uses the ground antennas to periodically upload the ephemeris and clock data to each satellite for re-transmission in the navigation message.

The user segment consists of individual radio receivers capable of receiving RF signals broadcasted by GPS satellites. These receivers catch, decode and process these signals to calculate a PVT solution. The ranging codes broadcast by the satellites enable a GPS receiver to measure the transit time of the signals and thereby determine the range between each satellite and the receiver. The navigation data message enables a receiver to calculate the position of each satellite at the time the signals were transmitted. The receiver then uses this information to determine its own PVT. At least 4 satellites are necessary in order for the receiver to find the 3 unknown position elements and the receiver clock error.

2.2.2 Pseudo and Delta-Range Measurements

GPS ranging signals (encoded in the received signal) that are transmitted by the satellites are used to measure the distance between the satellites and the receiver. These signals travel the line of sight path and when they come to the receiver, they are delayed by the amount of the range between the satellite and the user's antenna. This range can be shown in distance units as the time delay multiplied by the speed of light, c.

$$R = c.(T_{receive} - T_{transmit}) = c.\Delta T$$

This range is called pseudo-range because it cannot be measured exactly due to the errors resulting from receiver's clock bias, atmospheric delays, satellite clock bias, multi-path effects etc. The pseudo-range between the user and the satellite can be written in terms of these factors as follows:

$$PR = c.\Delta T + c.(b_r + b_s) + d_{iono} + d_{tropo} + \varepsilon_{multipath} + \varepsilon_{noise}$$

c	: speed of light
PR	: pseudo - range
ΔT	: signal time delay
b_r	: receiver clock bias error
b_s	: bias due to satellite clock error
d_{iono}	: ionospheric delay
d_{tropo}	: tropospheric delay
$\varepsilon_{multipath}$	: error due to multipath
ε_{noise}	: random noise

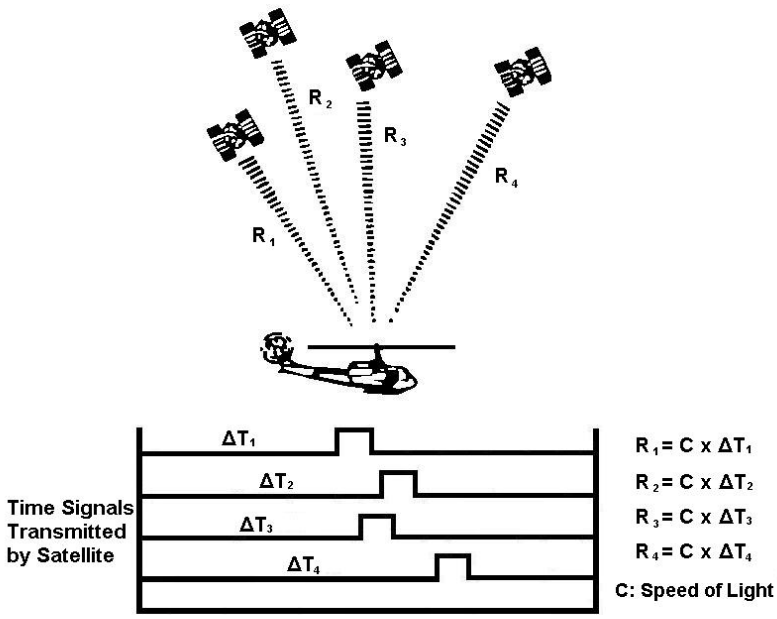

Figure 2-1 GPS Ranging Signals

The most important error on the pseudo-range is the receiver clock bias. The ranging procedure used in the GPS technology needs very accurate synchronization between the satellite and receiver clocks. GPS satellites use very accurate, stable and expensive atomic clocks but the receivers do not because it is economically infeasible. This problem is overcome by the following method: Besides the users unknown 3D coordinates, this error is removed by treating it as an additional unknown variable. We make use of one more additional satellite for this unknown variable so the total number of satellites needed for calculation increases to four.

The measured Doppler of the carrier signal can be used to determine the relative velocity between the satellite and the user. These are termed pseudo-range rate measurements and if they are integrated over regular time intervals we get what is called “delta-range”. The receiver uses Doppler measurements from at least 4 satellites to solve for the three dimensional velocity of the user and the receiver’s master oscillator frequency bias. Although this could be done by forming differences of pseudo-range based position estimates, frequency measurement is inherently much more accurate and has faster response in the presence of the user dynamics.

Delta-range measurements also carry some errors. The most relevant error is the receiver clock drift. A measured delta-range can be written as:

$$DR = c.\Delta T + c.\Delta T_{old} + b_d.\Delta t + \varepsilon_{noise}$$

c	: speed of light
DR	: delta - range
ΔT	: signal time delay at the end of integration interval
ΔT_{old}	: signal time delay at the start of integration interval
Δt	: measurement update interval
b_d	: bias due to receiver clock drift
ε_{noise}	: random noise

2.2.3 Ephemeris Data, Satellite Position Calculation

Ephemeris data is transmitted by GPS satellites and carried by the 'navigation message' part of the GPS signals. They include parameters to calculate satellite Earth Centered Earth Fixed (ECEF) frame positions with respect to time. Keplerian parameters describe the motion of the satellites in orbits and in the ephemeris data the values of these parameters are obtained via a least squares curve fit of the predicted ephemeris for the phase center of the satellite's antenna. Each satellite has its own set of ephemeris data and the ephemeris data is normally valid and can be used for precise navigation for a period of four hours following issue of a new data set by the satellite. The satellites transmit new ephemeris data every two hours which are determined by the master control station of the GPS Control Segment.

Ephemeris data is not enough for precise calculation, the calculated values should also be corrected for satellite clock-bias, ionospheric and tropospheric signal-propagation delays. Ephemeris data has also small errors causing corresponding errors in the computed position and velocity.

Measuring the pseudo-ranges, delta-ranges, correcting them for the ionospheric, tropospheric and clock error delays and calculating the satellite positions from the ephemeris data, we can now construct the GPS measurement equations.

2.2.4 GPS Measurement Equation and GPS Measurement Model

When a receiver has collected pseudo-range measurements, delta-range measurements, and navigation data from four (or more) satellites, it may calculate the navigation solution that is position, velocity, and time (PVT). Each navigation data message contains precise orbital (ephemeris) parameters for the transmitting satellite, enabling a receiver to calculate the position of each satellite at the time the signals were transmitted.

The receiver solves a minimum of four simultaneous pseudo-range equations, with the receiver 3D position and clock offset as the four unknown variables. Each equation is an expression of the principle that the true range (the difference between the pseudo-range and the receiver clock offset) is equal to the distance between the known satellite position and the unknown receiver position. The observation equations in three dimensions for each satellite with known coordinates and unknown user coordinates can be expressed mathematically by

$$\rho - \delta t_b = \left\| \mathbf{R}_r - \mathbf{R}_s \right\|_2 .$$

If there are k satellites, then corresponding to each of them we can write

$$\rho_i - \delta t_b = \sqrt{(x_r - x_{s_i})^2 + (y_r - y_{s_i})^2 + (z_r - z_{s_i})^2} + (\text{Meas. Noise})_i \qquad (2.1)$$

for $i = 1$ to k where

ρ_i : pseudo - range measurement
$\delta t_b = c.b_r$: receiver clock bias in meters
c : speed of light
x_{s_i} : x position of i^{th} satellite x_r : x position of receiver
y_{s_i} : y position of i^{th} satellite y_r : y position of receiver
z_{s_i} : z position of i^{th} satellite z_r : z position of receiver

$$\mathbf{R}_s = \begin{bmatrix} x_{s_i} \\ y_{s_i} \\ z_{s_i} \end{bmatrix} \qquad \mathbf{R}_r = \begin{bmatrix} x_r \\ y_r \\ z_r \end{bmatrix}$$

These are simplified versions of the equations actually used by GPS receivers. A receiver also obtains corrections derived from the navigation messages, which it applies to the pseudo-ranges. These include corrections for the satellite clock offset, relativistic effects, and ionospheric signal propagation delays.

The GPS measurement equation in 2.1 is non-linear and in order to develop a linear GPS measurement model we need to linearize it. Let the vector of ranges be $\mathbf{X}_\rho = [\rho_1 \ \ \rho_2 \ \ \cdots \ \ \rho_k]^T = \mathbf{h}(\mathbf{R})$, a non-linear function $\mathbf{h}(\mathbf{R})$ of the four dimensional vector $\mathbf{R} = [x_r \ \ y_r \ \ z_r \ \ \delta t_b]^T$ representing user position and receiver clock bias. We can express $\mathbf{X}_\rho$ hence ρ_i as a Taylor series expansion about a nominal value $\mathbf{X}_{nom}$ and ρ_{nom}.

$$\rho_i \cong \rho_{nom} + \frac{\partial \rho_i}{\partial x_r}\delta x_r + \frac{\partial \rho_i}{\partial y_r}\delta y_r + \frac{\partial \rho_i}{\partial z_r}\delta z_r + \delta t_b + \text{HOT}$$

rearranging,

$$\rho_i - \rho_{nom} \cong h_{i1}\delta x_r + h_{i2}\delta y_r + h_{i3}\delta z_r + \delta t_b + \text{HOT} \qquad \text{for } i = 1 \text{ to } k$$

where

$$h_{i1} = \left. \frac{-(x_{s_i} - x_r)}{\sqrt{(x_{s_i} - x_r)^2 + (y_{s_i} - y_r)^2 + (z_{s_i} - z_r)^2}} \right|_{x_r = x_{nom}},$$

$$h_{i2} = \left. \frac{-(y_{s_i} - y_r)}{\sqrt{(x_{s_i} - x_r)^2 + (y_{s_i} - y_r)^2 + (z_{s_i} - z_r)^2}} \right|_{y_r = y_{nom}}, \text{ and}$$

$$h_{i3} = \left. \frac{-(z_{s_i} - z_r)}{\sqrt{(x_{s_i} - x_r)^2 + (y_{s_i} - y_r)^2 + (z_{s_i} - z_r)^2}} \right|_{z_r = z_{nom}}.$$

These equations for $k = 4$ can be expressed in vector form as

$$\begin{bmatrix} \rho_1 - \rho_{nom} \\ \rho_2 - \rho_{nom} \\ \rho_3 - \rho_{nom} \\ \rho_4 - \rho_{nom} \end{bmatrix} \cong \begin{bmatrix} h_{11} & h_{12} & h_{13} & 1 \\ h_{21} & h_{22} & h_{23} & 1 \\ h_{31} & h_{32} & h_{33} & 1 \\ h_{41} & h_{42} & h_{43} & 1 \end{bmatrix} \begin{bmatrix} \delta x_r \\ \delta y_r \\ \delta z_r \\ \delta t_b \end{bmatrix}. \tag{2.2}$$

We add a noise term on the right hand side of the equation 2.2 due to the uncertainty in the GPS receiver measurements and write it in symbolic form as

$$\begin{aligned} &\delta \mathbf{X}_\rho = \mathbf{H}.\delta \mathbf{R} + \mathbf{v}_\rho \\ &\mathbf{v}_\rho \ : \text{noise in receiver measurements} \end{aligned}.$$

This set of equations can be solved by linear least squares method. Assuming that ρ_i's are the pseudo-ranges that are corrupted by noise, then the least square estimate of the unknown position and clock bias vector $\mathbf{R}$ is:

$$\delta \mathbf{R} = \left(\mathbf{H}^{\mathrm{T}} \mathbf{H}\right)^{-1} \mathbf{H}^{\mathrm{T}} \cdot \delta \mathbf{X}_\rho .$$

An iterative approach for the least square method can also be applied as follows. Start with an initial estimate for the nominal value and find the best estimate corresponding to this value. Then use this value as the next nominal point and find the next best estimate and go on like this until the estimate is smaller than a threshold value.

For completeness, we can write delta-range equations. Delta-ranges are the time derivatives of the pseudo-ranges and can be shown as:

$$\dot{\rho}_i = \frac{\left[(x_r - x_{s_i})(\dot{x}_r - \dot{x}_{s_i}) + (y_r - y_{s_i})(\dot{y}_r - \dot{y}_{s_i}) + (z_r - z_{s_i})(\dot{z}_r - \dot{z}_{s_i})\right]}{\rho_i}$$

$$\begin{aligned} &\dot{\rho}_i \ : \text{delta-range (known)} \\ &\rho_i \ : \text{pseudo-range (known)} \\ &(x_r, y_r, z_r) \ : \text{user position (known from position calculations)} \\ &(\dot{x}_r, \dot{y}_r, \dot{z}_r) \ : \text{user velocity (unknown)} \\ &(x_{s_i}, y_{s_i}, z_{s_i}) \ : \text{satellite positions (known)} \\ &(\dot{x}_{s_i}, \dot{y}_{s_i}, \dot{z}_{s_i}) \ : \text{satellite rate (known)} \end{aligned}$$

Defining,

$$\delta\dot{\rho}_i = \dot{\rho}_i - \dot{\rho}_{i_{nom}}$$

$$\delta\mathbf{V} = \begin{bmatrix} \delta V_x \\ \delta V_y \\ \delta V_z \end{bmatrix} = \begin{bmatrix} \dot{x}_r - \dot{x}_{r_{nom}} \\ \dot{y}_r - \dot{y}_{r_{nom}} \\ \dot{z}_r - \dot{z}_{r_{nom}} \end{bmatrix}$$

and linearizing the delta range equation about a nominal point, we can write the resulting equations in vector form as,

$$\begin{bmatrix} \delta\dot{\rho}_1 \\ \delta\dot{\rho}_2 \\ \delta\dot{\rho}_3 \\ \delta\dot{\rho}_4 \end{bmatrix} \cong \begin{bmatrix} h_{11} & h_{12} & h_{13} & 1 \\ h_{21} & h_{22} & h_{23} & 1 \\ h_{31} & h_{32} & h_{33} & 1 \\ h_{41} & h_{42} & h_{43} & 1 \end{bmatrix} \begin{bmatrix} \delta V_x \\ \delta V_y \\ \delta V_z \\ \delta t_d \end{bmatrix}$$

δt_d : receiver clock drift

In complete form, the GPS measurement model is given in equation 2.3 below:

$$\begin{bmatrix} \delta\rho_1 \\ \delta\rho_2 \\ \vdots \\ \delta\rho_n \\ \delta\dot{\rho}_1 \\ \delta\dot{\rho}_2 \\ \vdots \\ \delta\dot{\rho}_n \end{bmatrix} = \begin{bmatrix} h_{11} & h_{12} & h_{13} & 0 & 0 & 0 & 1 & 0 \\ h_{21} & h_{22} & h_{23} & 0 & 0 & 0 & 1 & 0 \\ \vdots & \vdots & \vdots & \vdots & \vdots & \vdots & \vdots & \vdots \\ h_{n1} & h_{n2} & h_{n3} & 0 & 0 & 0 & 1 & 0 \\ 0 & 0 & 0 & h_{11} & h_{12} & h_{13} & 0 & 1 \\ 0 & 0 & 0 & h_{21} & h_{22} & h_{23} & 0 & 1 \\ \vdots & \vdots & \vdots & \vdots & \vdots & \vdots & \vdots & \vdots \\ 0 & 0 & 0 & h_{n1} & h_{n2} & h_{n3} & 0 & 1 \end{bmatrix} \cdot \begin{bmatrix} \delta R_x \\ \delta R_y \\ \delta R_z \\ \delta V_x \\ \delta V_y \\ \delta V_z \\ \delta t_b \\ \delta t_d \end{bmatrix} + \begin{bmatrix} v_1 \\ v_2 \\ \vdots \\ v_n \\ v_{n+1} \\ v_{n+2} \\ \vdots \\ v_{2n} \end{bmatrix} \tag{2.3}$$

2.3 Inertial Navigation Systems

Navigation in basic words is traveling and finding the way from one place to another. These systems provide an operator or control system with the necessary information to effect some action in response to data provided by them. The main data produced is the position, velocity, attitude and time information. Another fact is that these systems work with respect to a reference system. Navigation systems are used for land, sea, airborne and space vehicles (Titterton and Weston (1997), Rogers (2000), Biezad (1999)).

Today, there are different kinds of navigation aids used throughout the world such as radio navigation systems GPS, LORAN, OMEGA; digital map systems, dead reckoning systems etc. The heart of all is a sensor to gather navigational information. Inertial navigation systems are the ones using inertial sensors for this purpose. The outgoing sections provide brief information on this subject matter.

2.3.1 Inertial Navigation Principles

An inertial navigation system utilizes data from force and inertial angular velocity sensors to determine necessary information. The main idea is based on the acceleration integrations. The first integration of the vehicle acceleration provides the velocity, and the second integration yields the vehicle position increments with respect to the initial point. In order to project the accelerations on the reference frame, angular velocities are integrated to give angular increments with respect to the initial attitude (Salychev (1998), Chatfield (1997)). As understood above, both positional and angular computations need the knowledge of initial values of position and orientation.

There are two types of implementation of an inertial navigation system: Stable Platform or Gimbaled Systems and Strapdown systems. Although the principle is same, implementation differs for both. For the Gimbaled systems inertial sensors are placed on a stable platform that is mechanically isolated from the motion of the vehicle. For the Strapdown systems, the sensors are mounted directly on the body of the vehicle rigidly so that they are called “Strapdown”. This study is dedicated on the strapdown systems.

Inertial Navigation System (INS) can indeed be thought of as a computer getting information from inertial sensors, doing mathematical computations and outputting results. The computations are really based on the Newton’s Second Law of motion. In Figure 2-2 below, basic calculation steps of a Strapdown INS is shown and details will be given in the proceeding sections.

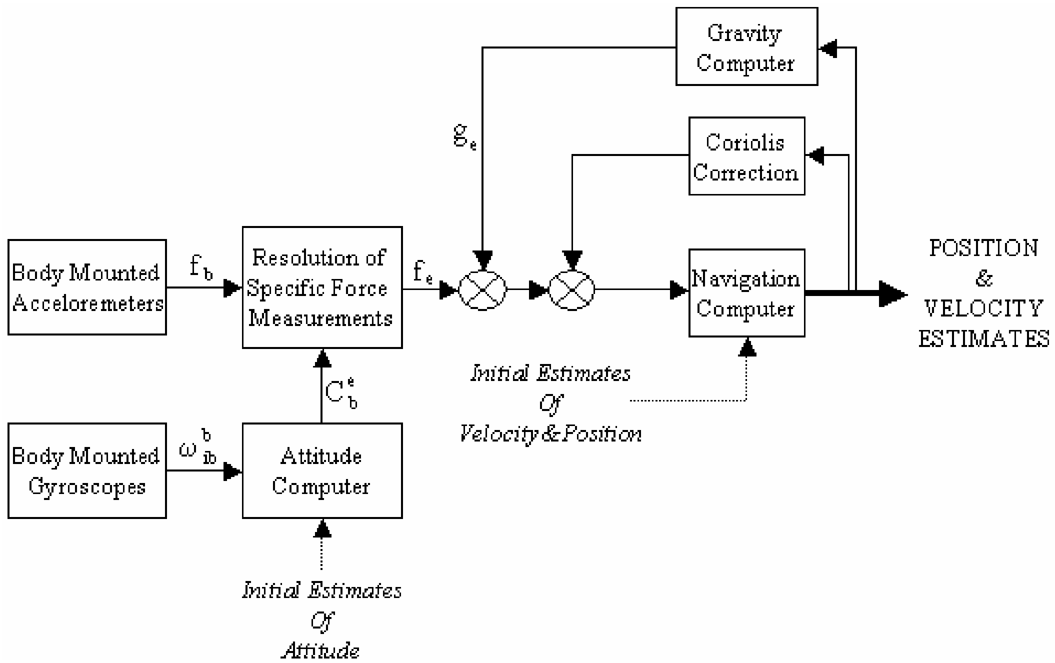

Figure 2-2 A Strapdown Inertial Navigation System Block Diagram

2.3.2 Inertial Sensors

Inside an INS, an accelerometer is used to measure the body accelerations and a gyroscope (often used as "gyro") is used to measure the angular velocity or directly the angle turned. An inertial measurement unit, or IMU, is a "clump" of six inertial sensors, three linear accelerometers and three rate gyros together with the supporting structure assembly and electronics.

Gyroscopes are used in various applications in a variety of roles such as flight path stabilization, autopilot feedback, sensor or platform stabilization and navigation. The most basic and the original form of the gyroscope make use of the inertial properties of a wheel, or rotor, spinning at high speed. A spinning wheel tends to maintain the direction of its spin axis in space by virtue of its angular momentum vector, the product of its inertia and spin speed, so defines a reference direction (Titterton and Weston (1997)). This principle guides through the basic Mechanical Gyro. With development in technology, many types of gyroscope architectures are developed. Nuclear Magnetic Resonance Gyros, Vibrating Gyros, Ring Laser Gyros, Fiber Optic Gyros, Solid State Gyros (MEMS) are some examples of current gyroscope technology.

An accelerometer uses the inertia of a mass to measure the difference between the kinematic acceleration with respect to inertial space and the gravitational acceleration. There are several principles that can form the basis for the design of an accelerometer. At its most basic level, an accelerometer can be viewed as a classical second order mechanical system; that is a damped mass-spring system under an applied force (Figure 2-3). When an accelerometer experiences acceleration, with a component parallel to its sensitive axis, the accelerometer's proof mass develops a corresponding inertial force ($f = m \cdot a$). This force acts on and displaces the spring a distance $x = f/k$ where k is the spring constant. The sensor's output is related either to the spring's displacement or to the spring's internal force, both of which are proportional to the applied acceleration. Some other accelerometer technologies can be summarized as: Pendulous Accelerometer, Solid State Accelerometer, and Fiber Optic Accelerometer.

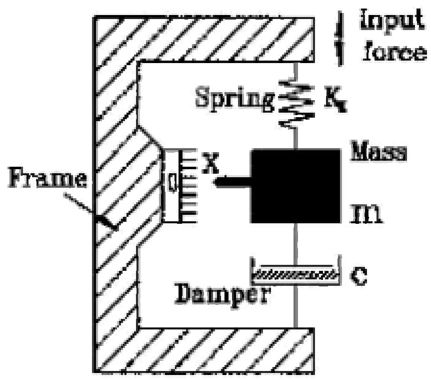

Figure 2-3 The Basic Accelerometer

The last thing to say about inertial sensors is that these sensors do not provide perfect measurements. They show different error characteristics according to their architecture and their grade. The errors in these sensors will be analyzed in section 2.3.6.

2.3.3 Reference Coordinate Frames

As mentioned before, a fundamental property of a navigation system is that it works with respect to a reference system. An INS uses accelerometers and gyro measurements referenced to an inertial frame, but navigation outputs are needed in a system referenced to earth. According to chosen reference system, sensor readings must be converted. In general, each frame has an orthogonal, right handed axis set and is defined by specifying the location of the origin and the direction of the three axes (Titterton and Weston (1997), Chatfield (1997)). The basic reference frames used through out this study is mentioned below.

2.3.3.1 Earth Centered Inertial Frame

Earth Centered Inertial Frame (ECI) has its origin at the mass center of the earth and it is non-rotating with respect to the distant stars. ECI defines an absolute space to which Newton's second law refers. So the inertial sensors measure specific forces with respect to these axes. In equations it is designated by a subscript $\mathbf{i}$. The orientation of the inertial coordinate axes is arbitrary. For inertial navigation purposes, the axes directions have been chosen such that the x_i and y_i inertial axes lie in the equatorial plane and the z_i axis is coincident with the earth's angular velocity vector. Because of the rotation of the earth, x_i and y_i does not remain fixed with respect to zero meridian.

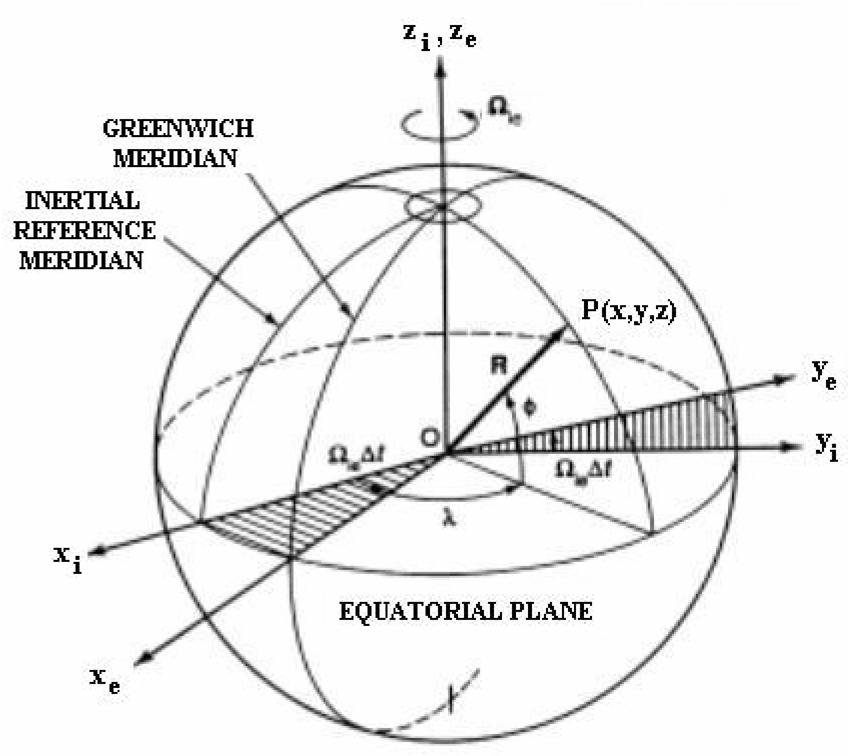

Figure 2-4 Earth Centered Inertial and Earth Centered Earth Fixed Frames

2.3.3.2 Earth Centered Earth Fixed Frame

Earth Centered Earth Fixed Frame (ECEF) has its origin at the mass center of the earth and it is non-rotating with respect to the earth. The ECEF frame rotates relative to the ECI frame at the rotation rate of the earth, ω_{ie}. In equations it is designated by a subscript $\mathbf{e}$. ECEF frame axis directions are defined as follows: x_e and y_e lies in the equatorial plane; x_e coincides with the zero meridian and y_e is 90° east of the x_e, and z_e axis is coincident with the earth's angular velocity vector.

2.3.3.3 Body Frame

The body frame has its origin at the mass center of the vehicle to which navigation system is mounted. The body frame constitutes the vehicle axis known as roll, pitch and yaw. In equations it is designated by a subscript $\mathbf{b}$. The axis directions are defined as roll axis – forward along the longitudinal axis of the vehicle; pitch axis – directed 90° to the right, normal to the roll axis; and yaw axis – directed downward normal to the roll – pitch plane. The origin of the body frame does not, in general, coincide with the location of the navigation system.

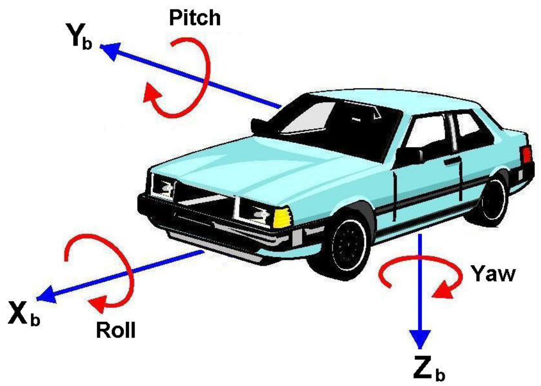

Figure 2-5 Body Frame

2.3.3.4 Inertial Sensor Frame

The inertial sensor frame is aligned with the three sensitive axes of the inertial measurement unit each is placed perpendicular to each other in a three axes system. The sensitive axis of each sensor describes an axis of the inertial sensor frame. The axis of the navigation system made up of this inertial measurement unit is described with this frame.

2.3.4 Inertial Navigation Equations

In this section, equations describing navigation states (position, velocity and attitude) for strapdown navigation system implementation referenced to Earth Centered Earth Fixed Frame (ECEF) are developed. In developing these equations, the objective is to form them in terms of sensed accelerations and turn rates. The resulting differential equations are nonlinear.

2.3.4.1 Notations and Basic Principles

A skew symmetric matrix is a square matrix that satisfies the identity

$$\mathbf{A} = -\mathbf{A}^T .$$

A skew symmetric matrix must have zeros on its diagonal. The general $3x3$ skew symmetric matrix is of the form:

$$\begin{bmatrix} 0 & a_{12} & a_{13} \\ -a_{12} & 0 & a_{23} \\ -a_{13} & -a_{23} & 0 \end{bmatrix}.$$

Any 3 dimensional vector $\boldsymbol{\omega} = \begin{bmatrix} \omega_x \\ \omega_y \\ \omega_z \end{bmatrix}$ can be represented in its skew symmetric matrix form as $\boldsymbol{\Omega} = \begin{bmatrix} 0 & -\omega_z & \omega_y \\ \omega_z & 0 & -\omega_x \\ -\omega_y & \omega_x & 0 \end{bmatrix}$

The cross product of two vectors can be written as a matrix – vector product using the skew symmetric forms as:

$$\boldsymbol{\Omega} \cdot \mathbf{v} = \boldsymbol{\omega} \times \mathbf{v} .$$

One of the important matrices used in inertial navigation is “direction cosine matrix (DCM)”. These matrices relate a vector’s components in one coordinate frame to another frame.

$$\mathbf{r}_b = \mathbf{C}_a^b \mathbf{r}_a$$

$\mathbf{r}_a$: vector in a - frame
$\mathbf{r}_b$: vector in b - frame
$\mathbf{C}_a^b$: Direction Cosine Matrix, DCM

A DCM satisfies

$\left|\mathbf{C}_a^b\right| = 1, \qquad \mathbf{C}_a^b = \left[\mathbf{C}_b^a\right]^{-1}, \qquad \left[\mathbf{C}_a^b\right]^T = \left[\mathbf{C}_a^b\right]^{-1}.$

Derivative of a DCM is

$\dot{\mathbf{C}}_a^b = \mathbf{C}_a^b \mathbf{W}_{ba}^a$ and $\dot{\mathbf{C}}_b^a = -\mathbf{W}_{ba}^a \, \mathbf{C}_b^a$ where

$\mathbf{W}_{ba}^a = \begin{bmatrix} 0 & -\omega_z & \omega_y \\ \omega_z & 0 & -\omega_x \\ -\omega_y & \omega_x & 0 \end{bmatrix}$ and it is the skew symmetric form of the vector

$\boldsymbol{\omega}_{ba}^a = \begin{bmatrix} \omega_x \\ \omega_y \\ \omega_z \end{bmatrix} \equiv$ angular velocity of a – frame wrt b – frame .

Here the superscript a in $\boldsymbol{\omega}_{ba}^a$ represents that this equation is expressed in a - frame and this notation is used throughout the thesis. If a subscript is not used it means that the operation on that vector can be done in any frame, or a frame is not chosen.

The similarity transformation $\mathbf{W}_{ba}^b = \mathbf{C}_a^b \mathbf{W}_{ba}^a \mathbf{C}_b^a$ for a DCM is also true.

Time derivative of a vector with respect to a reference frame is shown as

$$\left.\frac{d\mathbf{R}}{dt}\right|_i$$

where the subscript i on the derivation represents that this operation is done with respect to i frame. If this frame is rotating with respect to another frame, from the Coriolis equation one may relate the time derivative of a vector in one frame to another frame as

$$\underbrace{\left.\frac{d\mathbf{r}}{dt}\right|_i}_{\text{time derivative of } \mathbf{r} \text{ in } i \text{ coordinates}} = \underbrace{\left.\frac{d\mathbf{r}}{dt}\right|_b}_{\text{time derivative of } \mathbf{r} \text{ as seen by an observer in } b \text{ coordinates}} + \underbrace{\boldsymbol{\omega}_{ib} \times \mathbf{r}}_{\text{change in } \mathbf{r} \text{ caused by rotation of the } b \text{ frame}}$$

where $\boldsymbol{\omega}_{ib}$ is the turn rate of b frame with respect to i frame.

The equation 2.4 below is called the “Navigation Equation”. It says that total acceleration of a point in space is the sum of the total force acting on that point and the gravitational acceleration.

$$\left.\frac{d^2\mathbf{R}}{dt^2}\right|_i = \mathbf{f} + \mathbf{g} \tag{2.4}$$

Here $\mathbf{R}$ and $\mathbf{f}$ are any position and specific force vectors respectively and $\mathbf{g}$ is the gravity vector. The choice of the reference frame is critical here. This equation can be solved in any one of the navigation frames. For our purposes we write this equation in earth frame (ECEF):

$$\left.\frac{d^2\mathbf{R}_e}{dt^2}\right|_i = \mathbf{f}_e + \mathbf{g}_e \tag{2.5}$$

2.3.4.2 Velocity Equation

In this system, one needs to calculate the vehicle’s speed with respect to earth in Earth axis:

$$\mathbf{V}_e \equiv \left.\frac{d\mathbf{R}_e}{dt}\right|_e \tag{2.6}$$

$\mathbf{V}_e$: earth relative velocity of the vehicle
$\mathbf{R}_e$: position vector of vehicle with respect to earth's center
$\left.\frac{d\mathbf{R}_e}{dt}\right|_e$: rate of change of $\mathbf{R}_e$ with respect to ECEF coordinates

From the Coriolis equation, the rate of change of $\mathbf{V}_e$ may be expressed in terms of its rate of change in inertial coordinates as

$$\left.\frac{d\mathbf{V}_e}{dt}\right|_e = \left.\frac{d\mathbf{V}_e}{dt}\right|_i - \boldsymbol{\omega}_{ie}^e \times \mathbf{V}_e \tag{2.7}$$

where $\boldsymbol{\omega}_{ie}^e = \begin{bmatrix}0 & 0 & \omega_{ie}^e\end{bmatrix}^T$ is the turn rate of the earth with respect to the inertial frame expressed in earth frame and ω_{ie}^e is constant.

In order to calculate the first term on the right of the equation 2.7, we do the following:

$$\left.\frac{d\mathbf{R}_e}{dt}\right|_i = \left.\frac{d\mathbf{R}_e}{dt}\right|_e + \boldsymbol{\omega}_{ie}^e \times \mathbf{R}_e$$

Differentiating this expression with respect to time in inertial frame gives:

$$\left.\frac{d^2\mathbf{R}_e}{dt^2}\right|_i = \left.\frac{d\mathbf{V}_e}{dt}\right|_i + \dot{\boldsymbol{\omega}}_{ie}^e \times \mathbf{R}_e + \boldsymbol{\omega}_{ie}^e \times \left.\frac{d\mathbf{R}_e}{dt}\right|_i$$

Noting that:

$\left.\frac{d\mathbf{R}_e}{dt}\right|_i = \left.\frac{d\mathbf{R}_e}{dt}\right|_e + \boldsymbol{\omega}_{ie}^e \times \mathbf{R}_e$ and $\dot{\boldsymbol{\omega}}_{ie}^e = \mathbf{0}$ since earth is assumed to rotate at a constant speed, we can write

$$\left.\frac{d^2\mathbf{R}_e}{dt^2}\right|_i = \left.\frac{d\mathbf{V}_e}{dt}\right|_i + \boldsymbol{\omega}_{ie}^e \times \mathbf{V}_e + \boldsymbol{\omega}_{ie}^e \times \left[\boldsymbol{\omega}_{ie}^e \times \mathbf{R}_e\right]$$

Combining this equation with equation 2.5 and rearranging yields:

$$\left.\frac{d\mathbf{V}_e}{dt}\right|_i = \mathbf{f}_e - \boldsymbol{\omega}_{ie}^e \times \mathbf{V}_e + \mathbf{g}_e - \boldsymbol{\omega}_{ie}^e \times \left[\boldsymbol{\omega}_{ie}^e \times \mathbf{R}_e\right] \tag{2.8}$$

We define:

$$\mathbf{g}_l = \mathbf{g}_e - \boldsymbol{\omega}_{ie}^e \times \left[\boldsymbol{\omega}_{ie}^e \times \mathbf{R}_e\right] \tag{2.9}$$

Substituting equation 2.8 into 2.7 and using equation 2.9 yields:

$$\left.\frac{d\mathbf{V}_e}{dt}\right|_e = \mathbf{f}_e - 2\boldsymbol{\omega}_{ie}^e \times \mathbf{V}_e + \mathbf{g}_l$$

Since accelerometers measure the specific force in the body frame, we write $\mathbf{f}_e$ in terms of $\mathbf{f}_b$ and then we end up with our differential equation for velocity of the inertial navigation system.

$$\left.\frac{d\mathbf{V}_e}{dt}\right|_e = \mathbf{C}_b^e \mathbf{f}_b - 2\boldsymbol{\omega}_{ie}^e \times \mathbf{V}_e + \mathbf{g}_l \tag{2.10}$$

$\mathbf{C}_b^e$ in equation 2.10 is a time dependant direction cosine matrix that converts the measured specific force vector from body frame to earth frame. This DCM is updated continuously since the body frame is always rotating with respect to the earth frame. $\mathbf{C}_b^e$ can be expressed as the multiplication of two DCMs which are body to navigation ($\mathbf{C}_b^n$) and navigation to earth frame ($\mathbf{C}_n^e$) direction cosine matrices. $\mathbf{C}_b^n$ includes terms of φ, ϑ, and ξ that are respectively roll, pitch, and yaw angles and $\mathbf{C}_n^e$ includes terms of geodetic latitude ϕ, and longitude λ. These two DCMs are given as:

$$\mathbf{C}_b^n = \begin{bmatrix} \cos\vartheta.\cos\xi & -\cos\varphi.\sin\xi + \sin\varphi.\sin\vartheta.\cos\xi & \sin\varphi.\sin\xi + \cos\varphi.\sin\vartheta.\cos\xi \\ \cos\vartheta.\sin\xi & \cos\varphi.\cos\xi + \sin\varphi.\sin\vartheta.\sin\xi & -\sin\varphi.\cos\xi + \cos\varphi.\sin\vartheta.\sin\xi \\ -\sin\vartheta & \sin\varphi.\cos\vartheta & \cos\varphi.\cos\vartheta \end{bmatrix}$$

$$\mathbf{C}_n^e = \begin{bmatrix} -\sin\phi.\cos\lambda & -\sin\phi.\sin\lambda & \cos\phi \\ -\sin\lambda & \cos\lambda & 0 \\ -\cos\phi.\cos\lambda & -\cos\phi.\sin\lambda & -\sin\phi \end{bmatrix}$$

and $\mathbf{C}_b^e = \mathbf{C}_n^e \cdot \mathbf{C}_b^n$.

2.3.4.3 Attitude Equation

The attitude dynamics equation can be maintained as a direction cosine matrix differential equation.

Derivative of the $\mathbf{C}_b^e$ DCM satisfies the relationship:

$$\dot{\mathbf{C}}_b^e = \mathbf{C}_b^e \boldsymbol{\Omega}_{eb}^b \tag{2.11}$$

In equation 2.11, $\boldsymbol{\Omega}_{eb}^b$ is the skew-symmetric matrix form of the vector $\boldsymbol{\omega}_{eb}^b$, body turn rate vector with respect to Earth frame expressed at body frame. Since this vector includes the Earth rate besides the measured body rates, it can be written in terms of $\boldsymbol{\omega}_{ib}^{b} = [p \quad q \quad r]^{T}$, the body turn rate vector that gyroscopes measure and $\boldsymbol{\omega}_{ie}^{b}$, the Earth rate expressed in body frame:

$$\boldsymbol{\omega}_{eb}^{b} = \boldsymbol{\omega}_{ib}^{b} - \boldsymbol{\omega}_{ie}^{b} \tag{2.12}$$

Let $\boldsymbol{\Omega}_{ib}^{b}$ and $\boldsymbol{\Omega}_{ie}^{b}$ denote the skew symmetric matrix form of the vectors $\boldsymbol{\omega}_{ib}^{b}$ and $\boldsymbol{\omega}_{ie}^{b}$ respectively and

$$\boldsymbol{\Omega}_{ib}^{b} = \begin{bmatrix} 0 & -r & q \\ r & 0 & -p \\ -q & p & 0 \end{bmatrix}$$

Then substituting equation 2.12 into 2.11:

$$\dot{\mathbf{C}}_{b}^{e} = \mathbf{C}_{b}^{e}\left(\boldsymbol{\Omega}_{ib}^{b} - \boldsymbol{\Omega}_{ie}^{b}\right) \tag{2.13}$$

We convert $\boldsymbol{\Omega}_{ie}^{e}$ to $\boldsymbol{\Omega}_{ie}^{b}$ using the similarity transformation

$$\boldsymbol{\Omega}_{ie}^{b} = \mathbf{C}_{e}^{b}\boldsymbol{\Omega}_{ie}^{e}\mathbf{C}_{b}^{e} \tag{2.14}$$

where $\boldsymbol{\Omega}_{ie}^{e}$ is the skew-symmetric form of $\boldsymbol{\omega}_{ie}^{e}$.

Then, substituting equation 2.14 into 2.13 we get equation 2.15

$$\dot{\mathbf{C}}_{b}^{e} = \mathbf{C}_{b}^{e}\boldsymbol{\Omega}_{ib}^{b} - \boldsymbol{\Omega}_{ie}^{e}\mathbf{C}_{b}^{e}. \tag{2.15}$$

Our aim is to construct the differential equations of the inertial navigation system variables position, velocity and attitude. Of course, we tried to relate them to sensor readings $\boldsymbol{\omega}_{ib}^{b}$ and $\mathbf{f}_{b}$, body turn rate and specific force respectively. As a summary, the resulting non-linear differential equations are given by the equations 2.6, 2.10, and 2.15 for position, velocity, and attitude respectively and for clarity they are repeated below.

$$\left.\frac{d\mathbf{R}_{e}}{dt}\right|_{e} = \mathbf{V}_{e}$$

$$\left.\frac{d\mathbf{V}_e}{dt}\right|_e = \mathbf{C}_b^e \mathbf{f}_b - 2\boldsymbol{\omega}_{ie}^e \times \mathbf{V}_e + \mathbf{g}_l$$

$$\dot{\mathbf{C}}_b^e = \mathbf{C}_b^e \boldsymbol{\Omega}_{ib}^b - \boldsymbol{\Omega}_{ie}^e \mathbf{C}_b^e$$

2.3.4.4 Gravity Model

The expression of the gravity vector is different in ECEF compared to the navigation frame because of the way the ECEF frame is defined. In equation 2.5, gravity mass attraction vector $\mathbf{g}_e$ is expressed in the Earth frame and in equation 2.9, $\mathbf{g}_l$ is defined in terms of $\mathbf{g}_e$, $\boldsymbol{\omega}_{ie}^e$ and $\mathbf{R}_e$.

The gravity model used for this study is taken from Britting (1971) where $\mathbf{g}_e$ directly expresses the gravity components in ECEF as given below.

GM : Earth's Gravitational Constant (3986004.418×10^8 m^3/s^2)
a : Earth equatorial radius (6378137.0 meters)
C_2 : Second degree zonal harmonic ($-1.082629821313 \times 10^{-3}$)
$R_e = \left(R_x^2 + R_y^2 + R_z^2\right)^{1/2}$

$$\mathbf{g}_l = \mathbf{g}_e - \boldsymbol{\Omega}_{ie}^e \boldsymbol{\Omega}_{ie}^e \mathbf{R}_e$$

$\mathbf{g}_e = \begin{bmatrix} g_x \\ g_y \\ g_z \end{bmatrix}$, and the components of $\mathbf{g}_e$ are,

$$g_x = -\frac{GM}{R_e^3}\left(1 - \frac{3}{2}C_2\left(\frac{a}{R_e}\right)^2\left(1 - 5\left(\frac{R_z}{R_e}\right)^2\right)\right) \cdot R_x$$

$$g_y = -\frac{GM}{R_e^3}\left(1 - \frac{3}{2}C_2\left(\frac{a}{R_e}\right)^2\left(1 - 5\left(\frac{R_y}{R_e}\right)^2\right)\right) \cdot R_y$$

$$g_z = -\frac{GM}{R_e^3}\left(1 - \frac{3}{2}C_2\left(\frac{a}{R_e}\right)^2\left(3 - 5\left(\frac{R_z}{R_e}\right)^2\right)\right) \cdot R_z$$

So, the gravitational acceleration vector $\mathbf{g}_l$ can be written as:

$$\mathbf{g}_l = \begin{bmatrix} g_x + \omega_{ie}^2 R_x \\ g_y + \omega_{ie}^2 R_y \\ g_z \end{bmatrix},$$ since Earth's rotation has no contribution on z component of the gravitational acceleration.

So that we have defined the position, velocity and attitude equations for an inertial navigation system. The INS equations can be summarized as in Figure 2-6 below.

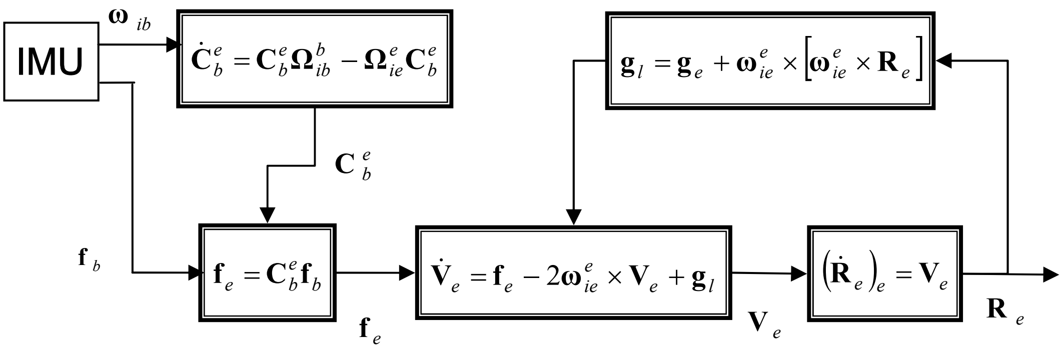

Figure 2-6 Inertial Navigation Equations Summary

2.3.5 INS Error Analysis

The nonlinear differential equations given in 2.6, 2.10 and 2.15 are the minimal equations necessary to calculate approximate INS solutions of a vehicle. In this section, the nonlinear navigation state equations are linearized to obtain linear error model. We use perturbation methods to linearize the non-linear system of differential equations. The whole system given in Figure 2-6 can be considered as an "estimation" of the true values of the outputs $\mathbf{R}_e$ and $\mathbf{V}_e$, so the state. Therefore the computed quantities that correspond to all the signals indicated in Figure 2-6 except $\boldsymbol{\omega}_{ib}$ and $\mathbf{f}_b$, are named as "estimates". Error equation is, by definition, the difference between the estimated and the true values of a variable say $\mathbf{x}$:

$$\delta\mathbf{x} = \hat{\mathbf{x}} - \mathbf{x},$$

where $\hat{\mathbf{x}}$ is the evaluated state vector and $\mathbf{x}$ is the true state vector.

When substitutions of the type above are made for dependant variables in the non-linear differential equations and products of error quantities are neglected, linear differential equations involving only the error quantities emerge (Britting, (1971)).

2.3.5.1 Attitude Error Propagation

Assume that the estimated earth axis is obtained from the true axis by rotations about the 3, 2, 1 axis by $d\alpha, d\beta, d\gamma$ amounts respectively. For small angles, the order of the rotation is not important and the relation between the estimated and the true Direction Cosine Matrix becomes:

$$\delta\mathbf{C}_b^e = \hat{\mathbf{C}}_b^e - \mathbf{C}_b^e = -\mathbf{\Psi}\mathbf{C}_b^e$$

$$\hat{\mathbf{C}}_b^e = [\mathbf{I} - \mathbf{\Psi}]\mathbf{C}_b^e \qquad (2.16)$$

Here, $\mathbf{\Psi}$ is the skew symmetric matrix formed from the vector $\boldsymbol{\psi} = [\delta\alpha \quad \delta\beta \quad \delta\gamma]^T$. For small $\delta\alpha$, $\delta\beta$, $\delta\gamma$; $[\mathbf{I} - \mathbf{\Psi}]$ is a transformation from true earth axis to estimated earth axis.

Linear differential equations governing the tilt error $[\delta\alpha \quad \delta\beta \quad \delta\gamma]^T$ angles can be derived as follows:

From equation 2.16,

$$\mathbf{\Psi} = \mathbf{I} - \hat{\mathbf{C}}_b^e \mathbf{C}_b^{e^T}$$

Differentiating this equation with respect to time we get,

$$\dot{\mathbf{\Psi}} = -\dot{\hat{\mathbf{C}}}_b^e \mathbf{C}_b^{e^T} - \hat{\mathbf{C}}_b^e \dot{\mathbf{C}}_b^{e^T} \tag{2.17}$$

From equation 2.15, differential equation for DCM is:

$$\dot{\mathbf{C}}_b^e = \mathbf{C}_b^e \mathbf{\Omega}_{ib}^b - \mathbf{\Omega}_{ie}^e \mathbf{C}_b^e$$
$$\dot{\hat{\mathbf{C}}}_b^e = \hat{\mathbf{C}}_b^e \hat{\mathbf{\Omega}}_{ib}^b - \mathbf{\Omega}_{ie}^e \hat{\mathbf{C}}_b^e$$

Here the assumption that $\dot{\mathbf{\Omega}}_{ie}^e = 0$ is used. Substituting these into equation 2.17 and using the fact that transpose of a skew-symmetric matrix is equal to its negative:

$$\dot{\mathbf{\Psi}} = -\left[\hat{\mathbf{C}}_b^e \hat{\mathbf{\Omega}}_{ib}^b - \mathbf{\Omega}_{ie}^e \hat{\mathbf{C}}_b^e\right]\mathbf{C}_b^{e^T} - \hat{\mathbf{C}}_b^e\left[\mathbf{C}_b^e \mathbf{\Omega}_{ib}^b - \mathbf{\Omega}_{ie}^e \mathbf{C}_b^e\right]^T$$
$$\dot{\mathbf{\Psi}} = -\hat{\mathbf{C}}_b^e \hat{\mathbf{\Omega}}_{ib}^b \mathbf{C}_b^{e^T} + \mathbf{\Omega}_{ie}^e \hat{\mathbf{C}}_b^e \mathbf{C}_b^{e^T} + \hat{\mathbf{C}}_b^e \mathbf{\Omega}_{ib}^b \mathbf{C}_b^{e^T} - \hat{\mathbf{C}}_b^e \mathbf{C}_b^{e^T} \mathbf{\Omega}_{ie}^e$$
$$\dot{\mathbf{\Psi}} = -\hat{\mathbf{C}}_b^e\left(\hat{\mathbf{\Omega}}_{ib}^b - \mathbf{\Omega}_{ib}^b\right)\mathbf{C}_b^{e^T} + \mathbf{\Omega}_{ie}^e \hat{\mathbf{C}}_b^e \mathbf{C}_b^{e^T} - \hat{\mathbf{C}}_b^e \mathbf{C}_b^{e^T} \mathbf{\Omega}_{ie}^e$$

Eliminating $\hat{\mathbf{C}}_b^e$ using equation 2.16 and letting $\delta\mathbf{\Omega}_{ib}^b = \hat{\mathbf{\Omega}}_{ib}^b - \mathbf{\Omega}_{ib}^b$ yields:

$$\dot{\mathbf{\Psi}} = -\left[\mathbf{I} - \mathbf{\Psi}\right]\mathbf{C}_b^e \delta\mathbf{\Omega}_{ib}^b \mathbf{C}_b^{e^T} + \mathbf{\Psi}\mathbf{\Omega}_{ie}^e - \mathbf{\Omega}_{ie}^e \mathbf{\Psi} \tag{2.18}$$

Using the properties of skew symmetric matrices and ignoring the multiplication of the error terms one may represent equation 2.18 in vector form as:

$$\dot{\boldsymbol{\psi}} = -\mathbf{C}_b^e \delta\boldsymbol{\omega}_{ib}^b - \mathbf{\Omega}_{ie}^e \boldsymbol{\psi} \tag{2.19}$$

2.3.5.2 Velocity Error Propagation

The differential equation satisfying the earth relative velocity was given in equation 2.10 as:

$$\left.\frac{d\mathbf{V}_e}{dt}\right|_e = \mathbf{C}_b^e \mathbf{f}_b - 2\boldsymbol{\omega}_{ie}^e \times \mathbf{V}_e + \mathbf{g}_l$$

and the relation between the estimated and the true values of $\mathbf{V}_e$ is:

$$\delta\mathbf{V}_e = \hat{\mathbf{V}}_e - \mathbf{V}_e \tag{2.20}$$

Taking derivatives of the both sides of equation 2.20 and using the differential equation satisfying the estimated value of $\mathbf{V}_e$ yields equation 2.21:

$$\delta\dot{\mathbf{V}}_e = \dot{\hat{\mathbf{V}}}_e - \dot{\mathbf{V}}_e$$

$$\dot{\mathbf{V}}_e = \mathbf{C}_b^e\mathbf{f}_b - 2\boldsymbol{\omega}_{ie}^e \times \mathbf{V}_e + \mathbf{g}_l$$
$$\dot{\hat{\mathbf{V}}}_e = \hat{\mathbf{C}}_b^e\hat{\mathbf{f}}_b - 2\boldsymbol{\omega}_{ie}^e \times \hat{\mathbf{V}}_e + \hat{\mathbf{g}}_l$$

$$\delta\dot{\mathbf{V}}_e = \hat{\mathbf{C}}_b^e\hat{\mathbf{f}}_b - 2\boldsymbol{\omega}_{ie}^e \times \hat{\mathbf{V}}_e + \hat{\mathbf{g}}_l - \mathbf{C}_b^e\mathbf{f}_b + 2\boldsymbol{\omega}_{ie}^e \times \mathbf{V}_e - \mathbf{g}_l \qquad (2.21)$$

Using equation 2.16 for $\hat{\mathbf{C}}_b^e$ and the below relations

$$\delta\mathbf{f}_b = \hat{\mathbf{f}}_b - \mathbf{f}_b$$
$$\delta\mathbf{g}_l = \hat{\mathbf{g}}_l - \mathbf{g}_l$$
$$\mathbf{f}_e = \mathbf{C}_b^e\mathbf{f}_b$$

we can write

$$\delta\dot{\mathbf{V}}_e = \mathbf{C}_b^e\delta\mathbf{f}_b - \boldsymbol{\Psi}\mathbf{f}_e - 2\boldsymbol{\Omega}_{ie}^e\delta\mathbf{V}_e + \delta\mathbf{g}_l$$

Using $skew(\mathbf{a})\cdot\mathbf{b} = -skew(\mathbf{b})\cdot\mathbf{a}$ property of the skew symmetric matrices we end with the error equation for velocity in vector form as

$$\delta\dot{\mathbf{V}}_e = \mathbf{C}_b^e\delta\mathbf{f}_b + \tilde{\mathbf{f}}_e\boldsymbol{\psi} - 2\boldsymbol{\Omega}_{ie}^e\delta\mathbf{V}_e + \delta\mathbf{g}_l \qquad (2.22)$$

In this equation $\tilde{\mathbf{f}}_e$ is the skew symmetric matrix form of $\mathbf{f}_e$, $\delta\mathbf{f}_b$ is the accelerometer bias error and $\delta\mathbf{g}_l$ is the error in the evaluation of the gravity vector. $\delta\mathbf{g}_l$ is given by

$$\delta\mathbf{g}_l = \delta\mathbf{g}_e - \boldsymbol{\omega}_{ie}^e \times [\boldsymbol{\omega}_{ie}^e \times \delta\mathbf{R}_e]$$

By definition gravity mass attraction vector $\mathbf{g}_e$ is:

$$\mathbf{g}_e = \mathbf{g}_0 + \Delta\mathbf{g} = -GM\cdot\mathbf{R}/R^3 + \Delta\mathbf{g}$$

where $\mathbf{g}_0$ is the spherical central force acceleration, $\Delta\mathbf{g}$ accounts for earth oblateness effects; GM is the earth's gravitational constant, and $R = \|\mathbf{R}_e\|_2$.

The gravity perturbation may then be expressed as

$$\delta\mathbf{g}_e = (\mathbf{G} + \Delta\mathbf{G}) \cdot \delta\mathbf{R}_e$$

where $\mathbf{G}$ and $\Delta\mathbf{G}$ are the gravity gradient matrices corresponding to $\mathbf{g}_0$ and $\Delta\mathbf{g}$ respectively. From Regan (1981) these are given by

$$\mathbf{G} = -\frac{GM}{R^3}\left[\mathbf{I} - 3\mathbf{u}_R\mathbf{u}_R{}^T\right]$$
$$\Delta\mathbf{G} = -\frac{3}{2}\frac{GM}{R^3}J_2\left(\frac{\mathbf{R}_e}{R}\right)^2\left[\mathbf{I} - 5\mathbf{u}_R\mathbf{u}_R{}^T\right]$$

where $\mathbf{u}_R$ is the unit vector in the direction of $\mathbf{R}_e$ and J_2 represents the oblate gravity potential second harmonic coefficient.

So we can write $\delta\mathbf{g}_l$ as:

$$\delta\mathbf{g}_l = \left(\mathbf{G} + \Delta\mathbf{G} - \mathbf{\Omega}_{ie}^e\mathbf{\Omega}_{ie}^e\right) \cdot \delta\mathbf{R}_e$$

The error equation for position is simply derived from equation 2.6 as:

$$\delta\dot{\mathbf{R}}_e = \delta\mathbf{V}_e \tag{2.23}$$

With perturbation of inertial navigation equations, we have ended up with linear differential equations of the basic inertial navigation state errors. As a summary, equations 2.23, 2.22, and 2.19 repeated below are linear error differential equations for position, velocity and attitude respectively.

$$\delta\dot{\mathbf{R}}_e = \delta\mathbf{V}_e$$
$$\delta\dot{\mathbf{V}}_e = \mathbf{C}_b^e\delta\mathbf{f}_b + \tilde{\mathbf{f}}_e\boldsymbol{\psi} - 2\mathbf{\Omega}_{ie}^e\delta\mathbf{V}_e + \delta\mathbf{g}_l$$
$$\dot{\boldsymbol{\psi}} = -\mathbf{C}_b^e\delta\boldsymbol{\omega}_{ib}^b - \mathbf{\Omega}_{ie}^e\boldsymbol{\psi}$$

We can express these equations in vector form as given below:

$$
\frac{d}{dt}\begin{bmatrix}\delta R_x\\ \delta R_y\\ \delta R_z\\ \delta V_x\\ \delta V_y\\ \delta V_z\\ \delta\alpha\\ \delta\beta\\ \delta\gamma\end{bmatrix}=\begin{bmatrix}0&0&0&1&0&0&0&0&0\\ 0&0&0&0&1&0&0&0&0\\ 0&0&0&0&0&1&0&0&0\\ \delta g_{11}+\omega_{ie}^2&0&0&0&2\omega_{ie}&0&0&-f_{ez}&f_{ey}\\ 0&\delta g_{22}+\omega_{ie}^2&0&-2\omega_{ie}&0&0&f_{ez}&0&-f_{ex}\\ 0&0&0&0&0&0&-f_{ey}&f_{ex}&0\\ 0&0&0&0&0&0&0&\omega_{ie}&0\\ 0&0&0&0&0&0&-\omega_{ie}&0&0\\ 0&0&0&0&0&0&0&0&0\end{bmatrix}\cdot\begin{bmatrix}\delta R_x\\ \delta R_y\\ \delta R_z\\ \delta V_x\\ \delta V_y\\ \delta V_z\\ \delta\alpha\\ \delta\beta\\ \delta\gamma\end{bmatrix}
$$

$$
+\begin{bmatrix}0&0&0&0&0&0\\ 0&0&0&0&0&0\\ 0&0&0&0&0&0\\ 0&0&0&&&\\ 0&0&0&&\mathbf{C}_b^e&\\ 0&0&0&&&\\ &&&0&0&0\\ &-\mathbf{C}_b^e&&0&0&0\\ &&&0&0&0\end{bmatrix}\cdot\begin{bmatrix}\left(\delta\omega_{ib}^b\right)_x\\ \left(\delta\omega_{ib}^b\right)_y\\ \left(\delta\omega_{ib}^b\right)_z\\ \left(\delta f_b\right)_x\\ \left(\delta f_b\right)_y\\ \left(\delta f_b\right)_z\end{bmatrix}
\tag{2.24}
$$

2.3.6 Sensor Errors

As mentioned before, all sensors are subject to errors which limit the accuracy of an inertial navigation system. Since these errors propagate through the other states of the system and create errors in the computed position, velocity, attitude etc, a vital part of the design and evaluation of integrated navigation systems is the ability to model and simulate errors associated with gyros and accelerometers (Grewal and Weill (2001), Rogers (2000)).

The measurement errors associated with inertial sensors are dependent on the physical operational principle of the sensor itself. Sensors are often compared on the basis of some errors like bias, scale factor, random noise etc. The major sources of errors for gyroscopes are fixed bias, acceleration dependant bias, scale factor errors, cross-coupling error, and misalignment errors. The major sources of errors for accelerometers are fixed bias, random bias, scale factor errors, cross-coupling error, and misalignment errors.

In general form, the output of an inertial sensor, an accelerometer or a gyroscope, can be written as:

$$\tilde{\mathbf{f}} = \mathbf{f} + \delta\mathbf{f}$$

where $\tilde{\mathbf{f}}$ is the measured sensor output, and $\delta\mathbf{f}$ is the measurement uncertainty.

The general error equation used for a gyroscope can be written as (Titterton and Weston (1997)):

$$\begin{bmatrix} \delta\omega_x \\ \delta\omega_y \\ \delta\omega_z \end{bmatrix} = \mathbf{b} + \mathbf{b}_g \begin{bmatrix} a_x \\ a_y \\ a_z \end{bmatrix} + \mathbf{S}_f \begin{bmatrix} \omega_x \\ \omega_y \\ \omega_z \end{bmatrix} + \mathbf{M} \begin{bmatrix} \omega_x \\ \omega_y \\ \omega_z \end{bmatrix} + \mathbf{w}$$

and that of accelerometers as:

$$\begin{bmatrix} \delta a_x \\ \delta a_y \\ \delta a_z \end{bmatrix} = \mathbf{b} + \mathbf{S}_f \begin{bmatrix} a_x \\ a_y \\ a_z \end{bmatrix} + \mathbf{M} \begin{bmatrix} a_x \\ a_y \\ a_z \end{bmatrix} + \mathbf{w}$$

where a_x, a_y, a_z are acting accelerations and $\omega_x, \omega_y, \omega_z$ are the acting angular rates, $\mathbf{b}$ is a three element vector representing the fixed biases which are present, $\mathbf{b}_g$ is a 3x3 matrix representing the g dependant bias coefficients, $\mathbf{S}_f$ is a diagonal matrix representing the scale factor errors, $\mathbf{M}$ is 3x3 skew symmetric matrix representing the mounting misalignment and cross-coupling terms and $\mathbf{w}$ is the random bias error.

In this study, reduced forms of the gyro and accelerometer error models which are only composed of the constant bias terms are used. In fact, using other components makes the system over-complex for a work of this kind which is a land navigation system. Inertial instrument errors can be modeled by random constants, random walk, random ramp or exponentially correlated random variables. For our purposes random walk model is used.

The state variable differential equation for the random walk process is (Gelb (1974))

$$\dot{\mathbf{x}} = \mathbf{w} \quad - \quad \text{Continuous form}$$
$$\mathbf{x}_{k+1} = \mathbf{x}_k + \mathbf{w}_k \quad - \quad \text{Discrete form} \tag{2.25}$$

where $\mathbf{w}$ and/or $\mathbf{w}_k$ are Gaussian white noise with $E[\mathbf{w}(t)\mathbf{w}(\tau)] = q(t)\delta(t-\tau)$ and $E[\mathbf{w}_k\mathbf{w}_l] = q_k\delta(k,l)$.

The random walk process results when uncorrelated signals are integrated and it varies randomly from one integration step to next (Gelb (1974), Chatfield (1997)). This model well suits the characteristics of the bias term for the inertial sensors. So using equation 2.25, the gyro and accelerometer bias errors can be defined in continuous time as

$$\begin{aligned} \delta\dot{\boldsymbol{\omega}}_b &= \mathbf{w}_g \\ \delta\dot{\mathbf{a}}_b &= \mathbf{w}_a \end{aligned} \tag{2.26}$$

With the light of this knowledge, we augment our state vector with error models of the gyroscope and the accelerometer and rewrite, in short notation, the linearized error equation in equation 2.24 driven by white noise $\mathbf{w}$ as:

$$\frac{d}{dt}\begin{bmatrix} \delta\mathbf{R}_e \\ \delta\mathbf{V}_e \\ \boldsymbol{\psi} \\ \delta\boldsymbol{\omega}_b \\ \delta\mathbf{a}_b \end{bmatrix} = \begin{bmatrix} \mathbf{0} & \mathbf{I} & \mathbf{0} & \mathbf{0} & \mathbf{0} \\ \delta\mathbf{g} - \boldsymbol{\Omega}_{ie}^e\boldsymbol{\Omega}_{ie}^e & -2\boldsymbol{\Omega}_{ie}^e & \mathbf{a}_e & \mathbf{0} & \mathbf{C}_b^e \\ \mathbf{0} & \mathbf{0} & -\boldsymbol{\Omega}_{ie}^e & -\mathbf{C}_b^e & \mathbf{0} \\ \mathbf{0} & \mathbf{0} & \mathbf{0} & \mathbf{0} & \mathbf{0} \\ \mathbf{0} & \mathbf{0} & \mathbf{0} & \mathbf{0} & \mathbf{0} \end{bmatrix} \cdot \begin{bmatrix} \delta\mathbf{R}_e \\ \delta\mathbf{V}_e \\ \boldsymbol{\psi} \\ \delta\boldsymbol{\omega}_b \\ \delta\mathbf{a}_b \end{bmatrix} + \mathbf{w} \tag{2.27}$$

2.4 Integrated Navigation Systems

In the early stages, GPS system was not intended to be used as a sole meaning of a navigation aid with high accuracy. But after the removal of the Selective Availability (SA) from GPS signals, developments in the “Differential GPS” and “Carrier Phase Positioning” concepts, it became a popular and an economic way of navigation. GPS still has problems from the point of view of accuracy, availability and integrity. Signal interruption is the main handicap affecting the availability. Blockage of the GPS antenna by the terrain conditions or indoor use of GPS or high dynamics of the host vehicle causes signal interruption and delay of the navigation outputs that can have severe implications and may not be tolerable for an accurate navigation system. Also low immunity of GPS signals to jamming signals in the environment places difficulties for navigation integrity. Another drawback of GPS is that it can not output vehicle attitude and acceleration.

The performance of an INS is characterized by a time dependant drift in the accuracy of the navigation output estimates that it provides. The rate at which navigation errors grow over long periods of time is governed predominantly by the accuracy of the knowledge of the initial position and attitude, imperfections in the inertial sensors and the dynamics of the trajectory followed by the host vehicle. Use of more accurate inertial sensors can improve performance but causes higher system costs (Titterton and Weston (1997)).

A recent approach to improve the INS accuracy is to employ some additional external information to correct navigation outputs. Basically, inertial navigation system outputs are compared with independent quantities derived from an external source (Titterton and Weston (1997)). A filter processes these outputs and estimates corrections of the navigation states. This is illustrated in Figure 2-7.

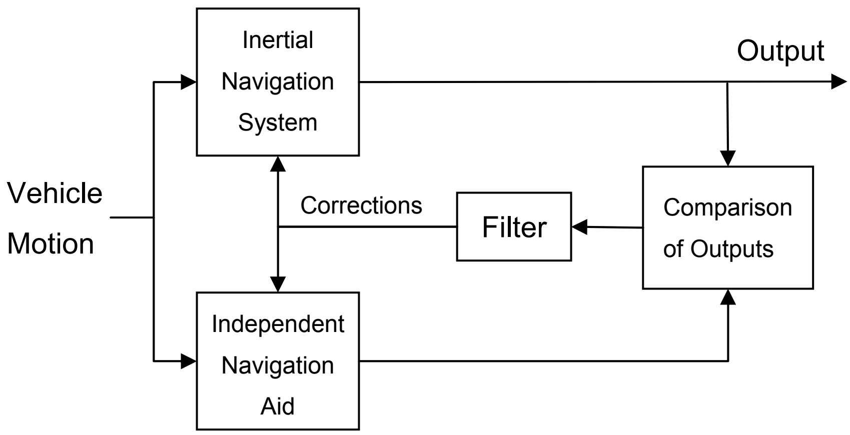

Figure 2-7 A Basic Form of an Integrated INS

The complementary characteristics of GPS make it a very favorable candidate for integration with INS. How the filter is structured within the navigation system depends on the types of sensors and model employed. For aided inertial navigation systems, the inertial component can either be an Inertial Measurement Unit (IMU), which only provides the raw acceleration and rotation rate data, or an

Inertial Navigation System (INS) providing position, velocity and attitude information. The aiding source can either be considered as a sensor providing raw sensor information, or as navigation system providing the position, velocity and/or attitude information. The model is constructed to estimate the principle states, position, velocity and attitude, or position, velocity and attitude errors of the vehicle.

2.4.1 Aided Inertial Navigation System Structures

The integration structure can vary with the feedback structure used or with the integration level realized. These examples cover “loosely coupled” and “tightly coupled” integration architectures. The term tightly coupled is usually applied to systems using single filter to integrate sensor data, whereas loosely coupled systems may contain more than one filter, but there are many possible levels of coupling between the extremes.

For either case, the observation delivered to the filter is the “observed error” of the inertial navigation solution, that is, the difference between the inertial navigation solution and the navigation solution provided by GPS. Since the observation is the observed error of the INS solution and since the filter is estimating the errors in the INS solution, the process model has to be in the form of an error model of the standard inertial navigation equations. Thus the inertial navigation equations are linearized to form error equations. Since the equations are linearized, the filter implementation takes on a linear form.

2.4.1.1 Loosely Coupled Integration

In the loosely coupled integration scheme, INS and GPS provide two independent sets of measurements of the vehicle state in the sense of independent navigators. INS is the main navigation aid and the measurements from the GPS are used to correct the INS errors. The filter operates on the difference of both navigation outputs. A direct feedback structure is used to online reset of INS errors as shown in Figure 2-8, but there is no feedback to the aiding sensor, GPS.

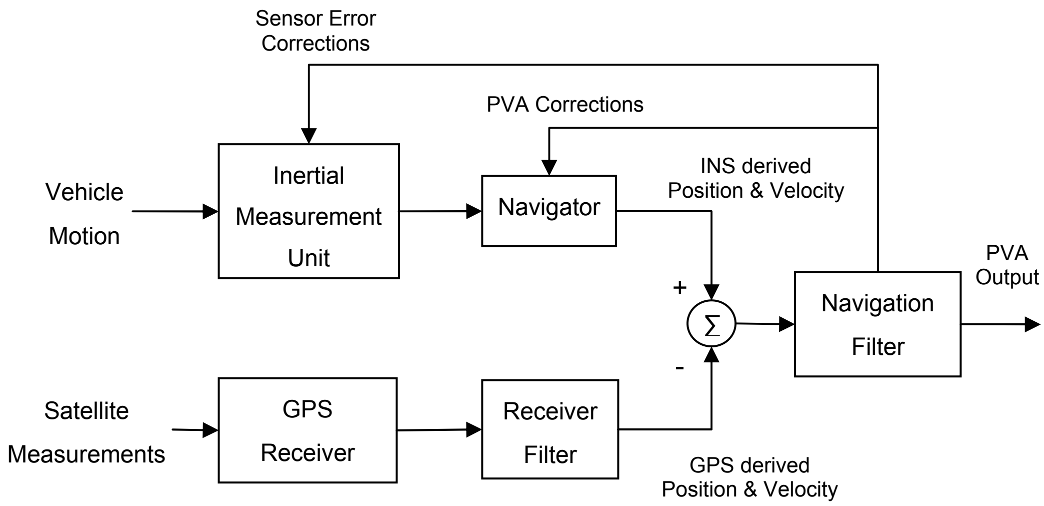

Figure 2-8 Loosely Coupled Integration Block Diagram

The disadvantages of the loosely coupled integration structure are:

- It is immune to the GPS position and velocity outputs. If GPS is not computing output (i.e. there are less than 4 satellites available) there is no aiding to the INS.
- The detection of jamming on GPS signals is not possible since the filter operates on GPS navigation outputs only.
- It can not help GPS to track satellites because there is no feedback to GPS.

The advantage of the loosely coupled configuration is being highly modular in accuracy and cost and ease of development since it is simpler.

2.4.1.2 Tightly Coupled Integration

In the tightly coupled integration scheme, both inputs are treated as sensors not as navigation systems. A filter integrates all measurements and estimates both IMU and GPS errors. Also a feedback is provided to the aiding source GPS to correct for the receiver clock bias and clock drift.

INS processes measurements from IMU and constructs the vehicle states, position velocity and attitude, in ECEF frame. The accuracy of the INS computations is improved by updating its output using GPS raw measurements that are pseudo and delta-ranges. To form the residual inputs to the navigation filter, a reconstruction of the pseudo-range and delta-range is made using INS – derived vehicle ECEF position and velocity and satellite ECEF positions based upon pre-loaded almanac data and they are differenced with the measured pseudo and delta-ranges from the GPS receiver. The filter estimates both vehicle state errors and GPS clock bias and drift errors. Then these error estimates are inserted at appropriate locations in the system in such a way as to cancel the effect of the error. The corrected INS data are better estimates of the true system navigation states. The resulting filter is nonlinear both in dynamics and measurements.

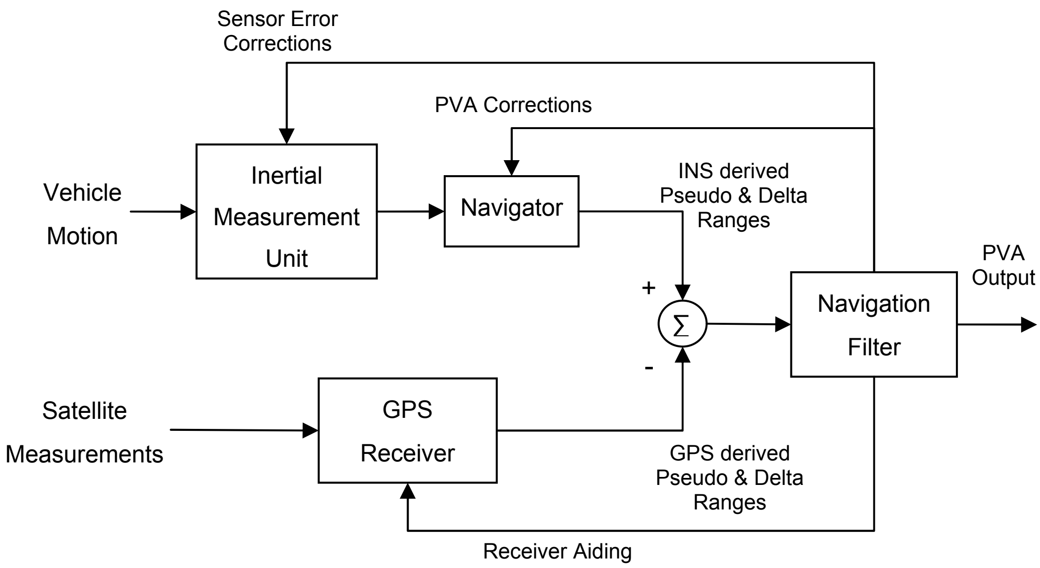

Figure 2-9 Tightly Coupled Integration Block Diagram

The advantages of the tightly coupled integration structure are:

- It is more robust and improves system integrity,
- Has superior performance compared to loosely coupled integration,
- Has more capability to reject jamming signals,

- Since raw measurements (pseudo and delta-range) are used, only one satellite can aid INS. GPS does not need to produce navigation outputs,
- Feedback to the GPS receiver helps GPS tracking loops.

The disadvantage of the tightly coupled integration is its being more expensive to implement and more difficult to develop.

2.4.2 Kalman Filtering

Kalman filter, from the point of view of this study, is a very famous algorithm for combining noisy sensor outputs to estimate the state of a system with uncertain dynamics. In more theoretical words, Kalman filter is a statistical recursive filter which provides an estimate of the states at time k given all observations up to time k. Kalman filter provides an optimal Minimal Mean Squared Error (MMSE) estimate of the states under certain conditions.

Kalman filter algorithm is used extensively in integrated navigation systems. With the application of this algorithm, independent redundant sources of navigation information are combined with a reference navigation solution to obtain an optimal estimate of navigation states – position, velocity and attitude – and other variables that contribute to navigation solution error (Rogers (2000)). For our purposes, the independent redundant source is the GPS measurements and the reference solution is the Inertial Navigation System's solution.

A central idea in the Kalman filter is to model the system of interest as a linear dynamic system which is excited by white noise and also whose sensors have error characteristics of a white noise. By knowing something about the nature of the noise (its first order statistics), it is possible to construct an optimal estimate of the system state even though the sensors are inexact. This is the fundamental idea of estimation theory. Without knowing the errors themselves, knowledge of their statistics allow construction of useful estimators based solely on that information.

A linear dynamic system driven by white noise can be stated in discrete time as follows:

$$\mathbf{x}(k) = \mathbf{F}(k)\mathbf{x}(k-1) + \mathbf{B}(k)\mathbf{u}(k) + \mathbf{w}(k) \tag{2.28}$$

where $\mathbf{x}(k)$ is the state vector of interest at time k, $\mathbf{F}(k)$ is a state transition matrix which relates the state vector from time $k-1$ to time k, $\mathbf{u}(k)$ is the controlled input vector while $\mathbf{B}(k)$ relates the control vector to the states and $\mathbf{w}(k)$ is the process noise injected into the system due to uncertainties in the transition matrix and control input.

The observation vector of this system is given by:

$$\mathbf{z}(k) = \mathbf{H}(k)\mathbf{x}(k) + \mathbf{v}(k) \tag{2.29}$$

where $\mathbf{H}(k)$ is the observation model relating the state vector at time k to the observation vector and $\mathbf{v}(k)$ is the observation noise vector which is related to the uncertainty in the observation.

Kalman filter puts some restrictions on this system that can be summarized as:

- Both process noise $\mathbf{w}(k)$ and the observation noise $\mathbf{v}(k)$ are assumed to be zero mean, Gaussian, uncorrelated random sequences with covariances:

$$\mathbf{E}\left[\mathbf{w}(i)\mathbf{w}^T(j)\right] = \begin{cases} \mathbf{Q}(k) & i = j = k \\ \mathbf{0} & i \neq j \end{cases}$$

$$\mathbf{E}\left[\mathbf{v}(i)\mathbf{v}^T(j)\right] = \begin{cases} \mathbf{R}(k) & i = j = k \\ \mathbf{0} & i \neq j \end{cases}$$

- It is assumed that the process and observation noises are uncorrelated:

$$\mathbf{E}\left[\mathbf{w}(i)\mathbf{v}(j)\right] = \mathbf{0}$$

- Initial estimates of the states and the state covariance matrix are known:

$$\mathbf{E}[\mathbf{x}_0] = \hat{\mathbf{x}}_0$$
$$\mathbf{E}\left[\tilde{\mathbf{x}}_0 \tilde{\mathbf{x}}_0^T\right] = \mathbf{P}_0$$

Through the proceeding sections, the algorithms which describe both the linear discrete and non-linear (extended) discrete Kalman filter will be given. The derivation of the algorithms which is out of our scope will not be given. The other forms of Kalman filter also will not be given here since our scope is the discrete and extended Kalman filter because of our INS and GPS models.

2.4.2.1 Discrete Kalman Filter

If the system process and measurement models are in the forms of equations 2.28 and 2.29, Kalman filter is designed in the discrete time. The design and development of filters in discrete time is a known and suitable situation for digital computers. The recursive nature of the Kalman filter let the designer to estimate the current value of the states without necessity to keep all the past measurements in the memory. In Table 2-1 below, the summary of the discrete Kalman filter equations are given (Gelb (1974)).

Table 2-1 Summary of Discrete Kalman Filter Equations

System Model Measurement Model	$\mathbf{x}_k = \mathbf{F}_{k-1}\mathbf{x}_{k-1} + \mathbf{w}_k, \quad \mathbf{w}_k \sim N(\mathbf{0}, \mathbf{Q}_k)$ $\mathbf{z}_k = \mathbf{H}_k \mathbf{x}_k + \mathbf{v}_k, \quad \mathbf{v}_k \sim N(\mathbf{0}, \mathbf{R}_k)$
Initial Conditions Other Assumptions	$E[\mathbf{x}(0)] = \hat{\mathbf{x}}_0, E\left[(\mathbf{x}(0) - \hat{\mathbf{x}}_0)(\mathbf{x}(0) - \hat{\mathbf{x}}_0)^T\right] = \mathbf{P}_0$ $E[\mathbf{w}_k \mathbf{v}_j] = 0$ for all j and k
State Estimate Extrapolation Error Covariance Extrapolation	$\hat{\mathbf{x}}_k(-) = \mathbf{F}_{k-1}\hat{\mathbf{x}}_{k-1}(+)$ $\mathbf{P}_k(-) = \mathbf{F}_{k-1}\mathbf{P}_{k-1}(+)\mathbf{F}_{k-1}{}^T + \mathbf{Q}_{k-1}$
State Estimate Update Error Covariance Estimate Kalman Gain Matrix	$\hat{\mathbf{x}}_k(+) = \hat{\mathbf{x}}_k(-) + \mathbf{K}_k\left[\mathbf{z}_k - \mathbf{H}_k\hat{\mathbf{x}}_k(-)\right]$ $\mathbf{P}_k(+) = [\mathbf{I} - \mathbf{K}_k\mathbf{H}_k]\mathbf{P}_k(-)$ $\mathbf{K}_k = \mathbf{P}_k(-)\mathbf{H}_k{}^T\left[\mathbf{H}_k\mathbf{P}_k(-)\mathbf{H}_k{}^T + \mathbf{R}_k\right]^{-1}$
Definitions	$\hat{\mathbf{x}}_k(-)$: state estimate at time k based on the measurements $\{\mathbf{z}_0, \ldots, \mathbf{z}_{k-1}\}$ $\mathbf{P}_k(-)$: Covariance matrix of $\hat{\mathbf{x}}_k(-)$ $\hat{\mathbf{x}}_k(+)$: state estimate at time k based on the measurements $\{\mathbf{z}_0, \ldots, \mathbf{z}_k\}$ $\mathbf{P}_k(+)$: Covariance matrix of $\hat{\mathbf{x}}_k(+)$ $\mathbf{K}_k$: Kalman gain matrix

2.4.2.2 Extended Kalman Filter

In most real cases the process and/or observation models do not behave linearly and hence the linear Kalman filter described above cannot be implemented. To overcome this, the extended Kalman filter (EKF) is developed (Gelb (1974)). It provides the best MMSE estimate of the state and in principle it is a linear estimator which linearizes the process and observation models about the current estimated state.

The main difference of the EKF is that the Kalman gain matrix of the EKF is a random function of the estimated state. The estimated states are used to build up the system matrix and the system matrix effects the Kalman gain matrix.

The non-linear discrete time system is described as

$$\mathbf{x}(k) = \mathbf{f}\big(\mathbf{x}(k-1), \mathbf{u}(k), k\big) + \mathbf{w}(k)$$

where $\mathbf{f}(\cdot,\cdot,k)$ is a non-linear state transition function at time k which forms the current state from the previous state and the current control input.

The non-linear observation model is represented as

$$\mathbf{z}(k) = \mathbf{h}\big(\mathbf{x}(k)\big) + \mathbf{v}(k)$$

In Table 2-1 below, the summary of the discrete Kalman filter equations are given (Gelb (1974)).

Table 2-2 Summary of Discrete Extended Kalman Filter Equations

System Model Measurement Model	$\mathbf{x}_k = \mathbf{f}(\mathbf{x}_{k-1}, k) + \mathbf{w}_k, \quad \mathbf{w}_k \sim N(\mathbf{0}, \mathbf{Q}_k)$ $\mathbf{z}_k = \mathbf{h}(\mathbf{x}_k) + \mathbf{v}_k, \quad \mathbf{v}_k \sim N(\mathbf{0}, \mathbf{R}_k)$
Initial Conditions Other Assumptions	$E[\mathbf{x}(0)] = \hat{\mathbf{x}}_0, E[(\mathbf{x}(0) - \hat{\mathbf{x}}_0)(\mathbf{x}(0) - \hat{\mathbf{x}}_0)^T] = \mathbf{P}_0$ $E[\mathbf{w}_k \mathbf{v}_j] = 0$ for all j and k
State Estimate Extrapolation Error Covariance Extrapolation	$\hat{\mathbf{x}}_{k+1}(-) = \mathbf{f}(\hat{\mathbf{x}}_k(+), k)$ $\mathbf{P}_{k+1}(-) = \mathbf{F}_k \mathbf{P}_k(+) \mathbf{F}_k^T + \mathbf{Q}_k$
State Estimate Update Error Covariance Estimate Kalman Gain Matrix	$\hat{\mathbf{x}}_k(+) = \hat{\mathbf{x}}_k(-) + \mathbf{K}_k[\mathbf{z}_k - \mathbf{h}_k(\hat{\mathbf{x}}_k(-))]$ $\mathbf{P}_k(+) = [\mathbf{I} - \mathbf{K}_k \mathbf{H}_k] \mathbf{P}_k(-)$ $\mathbf{K}_k = \mathbf{P}_k(-) \mathbf{H}_k^T [\mathbf{H}_k \mathbf{P}_k(-) \mathbf{H}_k^T + \mathbf{R}_k]^{-1}$
Definitions	$\mathbf{F}_k = \left.\dfrac{\partial \mathbf{f}(\mathbf{x}_k, k)}{\partial \mathbf{x}_k}\right\|_{\mathbf{x}_k = \hat{\mathbf{x}}_k}$ $\mathbf{H}_k = \left.\dfrac{\partial \mathbf{h}_k(\mathbf{x}_k)}{\partial \mathbf{x}_k}\right\|_{\mathbf{x}_k = \hat{\mathbf{x}}_k}$

2.4.2.3 Navigation Kalman Filter Implementation

We see that Kalman filter is based on linear system models derived by white noise. So we can use our linearized INS error equations derived in section 2.3.5 as the system dynamics model and GPS measurement equation derived in section 2.2.4 as the system measurement model.

The linearized INS error equation in 2.24 is combined with the sensor error model given in equation 2.26 to from the system dynamics model given by the equation 2.27 in which the system is derived by the white noise. The matrix equation is given in the short notation form where $\mathbf{R}_e$, $\mathbf{V}_e$ and $\mathbf{\Psi}$ are the three dimensional position, velocity and attitude vectors respectively; $\boldsymbol{\omega}_b$ and $\mathbf{a}_b$ are the three dimensional gyroscope and accelerometer bias vectors, t_b and t_d are the clock bias and the clock drift states respectively. $\mathbf{w}$ is the 17x1 system process noise composed of the position, velocity, attitude, gyro, accelerometer, clock drift and bias plant noises.

$$\frac{d}{dt}\begin{bmatrix} \delta\mathbf{R}_e \\ \delta\mathbf{V}_e \\ \boldsymbol{\psi} \\ \delta\boldsymbol{\omega}_b \\ \delta\mathbf{a}_b \\ \delta t_b \\ \delta t_d \end{bmatrix} = \begin{bmatrix} \mathbf{0} & \mathbf{I} & \mathbf{0} & \mathbf{0} & \mathbf{0} & \mathbf{0} & \mathbf{0} \\ \boldsymbol{\delta}\mathbf{g} - \mathbf{\Omega}_{ie}^{e}\mathbf{\Omega}_{ie}^{e} & -2\mathbf{\Omega}_{ie}^{e} & \mathbf{a}_e & \mathbf{0} & \mathbf{C}_b^e & \mathbf{0} & \mathbf{0} \\ \mathbf{0} & \mathbf{0} & -\mathbf{\Omega}_{ie}^{e} & -\mathbf{C}_b^e & \mathbf{0} & \mathbf{0} & \mathbf{0} \\ \mathbf{0} & \mathbf{0} & \mathbf{0} & \mathbf{0} & \mathbf{0} & \mathbf{0} & \mathbf{0} \\ \mathbf{0} & \mathbf{0} & \mathbf{0} & \mathbf{0} & \mathbf{0} & \mathbf{0} & \mathbf{0} \\ \mathbf{0} & \mathbf{0} & \mathbf{0} & \mathbf{0} & \mathbf{0} & \mathbf{0} & \mathbf{1} \\ \mathbf{0} & \mathbf{0} & \mathbf{0} & \mathbf{0} & \mathbf{0} & \mathbf{0} & \mathbf{0} \end{bmatrix} \cdot \begin{bmatrix} \delta\mathbf{R}_e \\ \delta\mathbf{V}_e \\ \boldsymbol{\psi} \\ \delta\boldsymbol{\omega}_b \\ \delta\mathbf{a}_b \\ \delta t_b \\ \delta t_d \end{bmatrix} + \mathbf{w} \qquad (2.30)$$

In general, the linearized form of the measurement equation is written as

$$\hat{\mathbf{z}}_k - \mathbf{z}_k = \delta\mathbf{z} = \mathbf{H}_k\delta\mathbf{x} + \mathbf{v}_k \qquad (2.31)$$

where $\hat{\mathbf{z}}_k$ is the predicted value of the output $\mathbf{z}$, and $\mathbf{v}_k$ is the measurement noise and is assumed to be white Gaussian and $\mathbf{H}_k = \left.\frac{\delta\mathbf{z}(t)}{\delta\mathbf{x}(t)}\right|_{\mathbf{x}=\hat{\mathbf{x}}}$.

GPS measurement equation given in equation 2.3 is also in the above form and can be written as below:

$$\begin{bmatrix} \delta\boldsymbol{\rho} \\ \delta\Delta\boldsymbol{\rho} \end{bmatrix} = \begin{bmatrix} \mathbf{h} & \mathbf{0} & \mathbf{0} & \mathbf{0} & \mathbf{0} & \mathbf{1} & \mathbf{0} \\ \mathbf{0} & \mathbf{h} & \mathbf{0} & \mathbf{0} & \mathbf{0} & \mathbf{0} & \mathbf{1} \end{bmatrix} \cdot \begin{bmatrix} \delta\mathbf{R}_e \\ \delta\mathbf{V}_e \\ \boldsymbol{\psi} \\ \delta\boldsymbol{\omega}_b \\ \delta\mathbf{a}_b \\ \delta t_b \\ \delta t_d \end{bmatrix} + \begin{bmatrix} \mathbf{v}_\rho \\ \mathbf{v}_{\Delta\rho} \end{bmatrix} \qquad (2.32)$$

In this equation, $\delta\boldsymbol{\rho}$ is the difference between the pseudo-ranges estimated in INS and measured by GPS; $\delta\boldsymbol{\Delta\rho}$ is the difference between the delta-ranges estimated in INS and measured by GPS; $\mathbf{v}_{\rho}$ and $\mathbf{v}_{\Delta\rho}$ are the added pseudo and delta-range measurement noises respectively.

Figure 2-10 summarizes the steps involved in the navigation Kalman filter implementation. The body-turn rates and body specific forces which are delivered by the Inertial Measurement Unit (IMU) are fed to the navigation equations in order to calculate the earth referenced acceleration, velocity and position. The position output of INS and satellite position calculated from the ephemeris data are used to calculate INS derived pseudo and delta-ranges. These are differenced with the measured pseudo and delta-range from the GPS receiver to construct the measurement residuals for the Kalman filter. The Kalman filter estimates the optimal errors for the states. The filter error estimates are then fed back to the appropriate points in the system in order to cancel the errors raised in the INS. The IMU output is corrected using the gyro and accelerometer bias filter estimates. The body to ECEF direction cosine matrix (DCM) is corrected using the body attitude error state. The ECEF position is corrected using the position error state. The earth relative velocity is corrected using the velocity error state. The receiver clock errors are compensated in the pseudo-range/delta-range reconstruction using the clock error states.

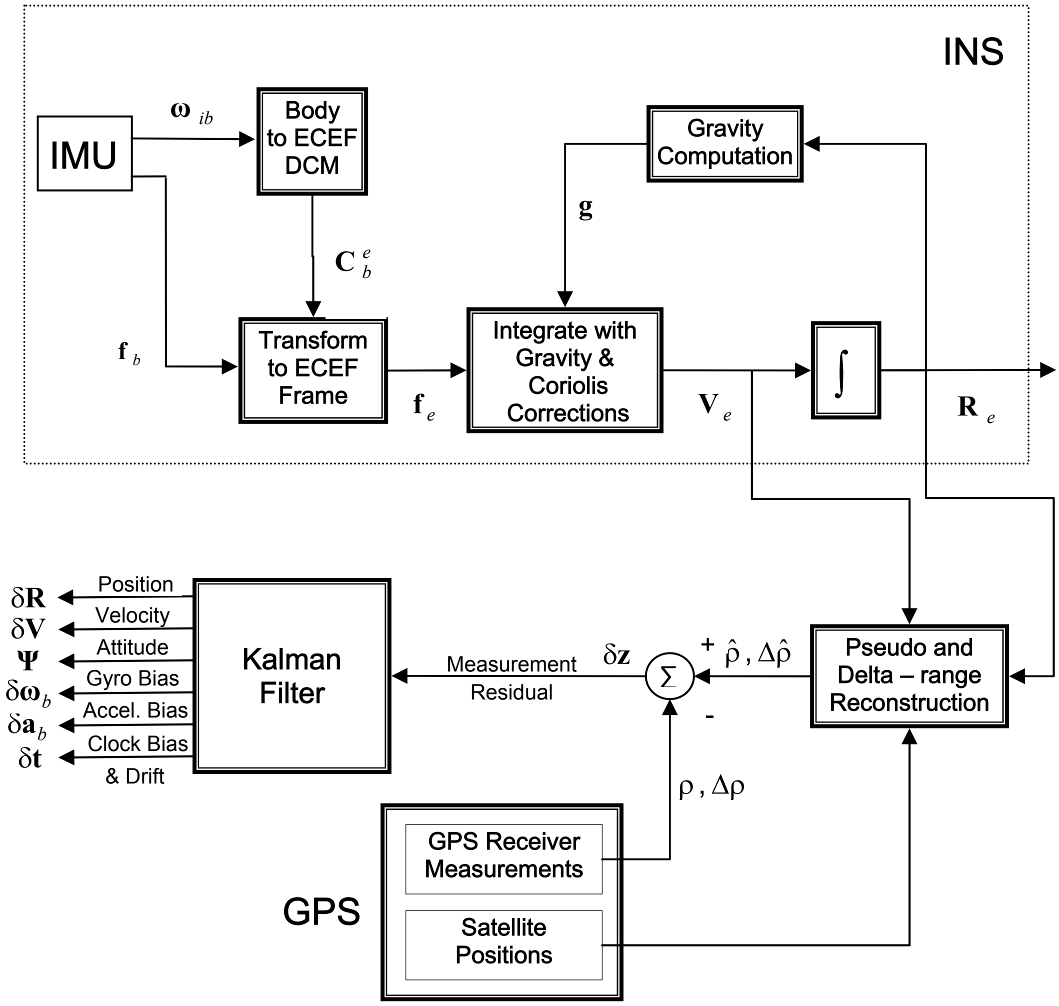

Figure 2-10 Navigation Kalman Filter Implementation

CHAPTER 3

OBSERVABILITY ANALYSIS

3.1 Introduction

The concept of observability comprises solving the problem of reconstructing unmeasurable state variables from measurable signals in a finite time interval. Integration of INS with other navigation aids can be considered as a stochastic “observer design” problem. So understanding observability concepts plays an important role on the success of the integration.

One of the main reasons for the observability analysis of a dynamic system is the need to determine the efficiency of Kalman filter designed to estimate the state of that system. The ability to estimate the state of a completely observable system depends only on the system driving noise and measurement noise. On the other hand, if the system is not observable, we cannot obtain an accurate estimate of the state even if the noise level is zero. In other words, the measure of observability sets a lower limit on the estimation error, and the lower the limit, the better is the chance to obtain an accurate estimate of the system states.

In this thesis work, the observability of the aided INS is examined based on the idea taken from the recent work of Koyaz (2003). In that work, aided INS is investigated from control theory point of view. A quantitative observability measure is derived based on the theoretical knowledge on linear systems and observability Gramian. This observability measure is tested on ideal fictitious scenarios of inertial navigation system.

In this chapter, useful topics exposing the observability concepts are given first. The definitions of observability, observability Gramian and observability measure are put forward. Then the observability analysis of the aided INS is explained based on the given introduction. Finally, the computation method of the observability measure for this study is described.

3.2 Observability Concepts

For the observability of linear systems, the unforced system described by equation 3.1 is used. In this equation, $\mathbf{x}(t)$ is the n – dimensional system state vector, $\mathbf{y}(t)$ is the m – dimensional output vector, $\mathbf{A}(t)$ and $\mathbf{C}(t)$ are $n \times n$ and $m \times n$ matrices respectively. The driving forces have no effect on the system observability since if the system defined by $(\mathbf{A},\mathbf{C})$ is not observable, then we cannot obtain an accurate estimate of the error state whatever the control vectors are.

$$\begin{aligned} &\dot{\mathbf{x}}(t) = \mathbf{A}(t) \cdot \mathbf{x}(t), \qquad \mathbf{x}(t_0) = \mathbf{x}_0 \\ &\mathbf{y}(t) = \mathbf{C}(t) \cdot \mathbf{x}(t) \end{aligned} \tag{3.1}$$

The linear state equation 3.1 is said to be observable on $\lfloor t_0, t_f \rfloor$ if any initial state $\mathbf{x}(t_0) = \mathbf{x}_0$ can uniquely be determined by the corresponding response $\mathbf{y}(t)$ for $t \in \lfloor t_0, t_f \rfloor$. If all states $\mathbf{x}(t)$ corresponding to all $\mathbf{y}(t)$ are observable, the system is completely observable.

While the observability condition for a time invariant system is rather simple, the condition of a time varying system is quite cumbersome and involves the concept of “observability Gramian”. The matrix $\mathbf{M}$ satisfying equation 3.2, where $\mathbf{\Phi}$ is the state transition matrix for the system in equation 3.1, is called the observability Gramian associated with time interval $\lfloor t_0, t_f \rfloor$.

$$\mathbf{M}(t_0, t_f) = \int_{t_0}^{t_f} \mathbf{\Phi}'(t, t_0)\mathbf{C}'(t)\mathbf{C}(t)\mathbf{\Phi}(t, t_0)dt \tag{3.2}$$

The following statement relates observability to observability Gramian: The system given in equation 3.1 is completely observable on the interval $\lfloor t_0, t_f \rfloor$, if and only if $\mathbf{M}(t_0, t_f)$ is positive definite, in other words it is nonsingular.

Next is to define physically meaningful measures for the observability. The following equation can be used as the degree of observability of a system if $\mathbf{M}(t_0, t_f)$ is nonsingular (Koyaz (2003)).

$$M_o \equiv \left\| \mathbf{M}(t_0, t_f)^{-1} \right\|^{-1} \tag{3.3}$$

In equation 3.3, $\mathbf{M}(t_0, t_f)$ is the observability Gramian. Since, the observability Gramian matrices are finite dimensional, without loss of generality, we can use any matrix norm to define the degree of observability. Among these norms, the Frobenious norm for any matrix $\mathbf{X}$ is defined as:

$$\|\mathbf{X}\|_F = \left[tr\left(\mathbf{X}^T \cdot \mathbf{X}\right)\right]^{1/2} .$$

Using the definition above for the Frobenious norm, observability measure M_o can be written as (Koyaz (2003)):

$$M_o = \left\|\mathbf{M}^{-1}\right\|_F^{-1} = \frac{1}{\left[tr\left(\left[\mathbf{M}^{-1}\right]^T \left[\mathbf{M}^{-1}\right]\right)\right]^{1/2}} . \tag{3.4}$$

Depending on the definition of observability measure given above, if the system in equation 3.1 is not observable then $M_o = 0$. Let M_o^a and M_o^b denote the observability measures for two different output structures. If $M_o^a > M_o^b$, then we say that system model a is more observable than model b. This simple remark summarizes the main approach in the observability analysis of the aided inertial navigation system (Koyaz (2003)).

3.3 Observability of the GPS/INS System

In this section, we will emphasize on the aided inertial navigation system representation from control theory point of view. For this purpose, we will use our linearized INS and GPS models derived in CHAPTER 2 and rearrange them to construct our representation. Then the computation method of the observability measure in our study will be given in detail.

3.3.1 Aided INS Representation

As mentioned before inertial navigation system is a computational mechanism which receives input from gyroscopes and accelerometers and outputs navigation states that are position, velocity, and attitude. Due to the nature of the INS, these computations are not exact and exhibit errors growing with time because of sensor errors, initial state uncertainties, equation uncertainties as well as computation errors arising from computer round offs and real time implementation inadequacies. These errors make INS an unstable system. Despite of these errors, we have something to do because we have knowledge on how they propagate. We develop an error model of the INS so that we can dynamically know their propagation in time. One other thing is that, if we have information about these navigation states from an independent external source, we can use those measurements to bound the errors in INS. Since we have a model of the error in INS, an observer can estimate the unknown errors in the system. The input to the observer is the difference between the INS navigation outputs and the measured outputs from the external source. The error estimates of this observer are fed back to the system to cancel the errors in the INS and this approach as a result stabilizes INS. This representation can be summarized with Figure 3-1 below.

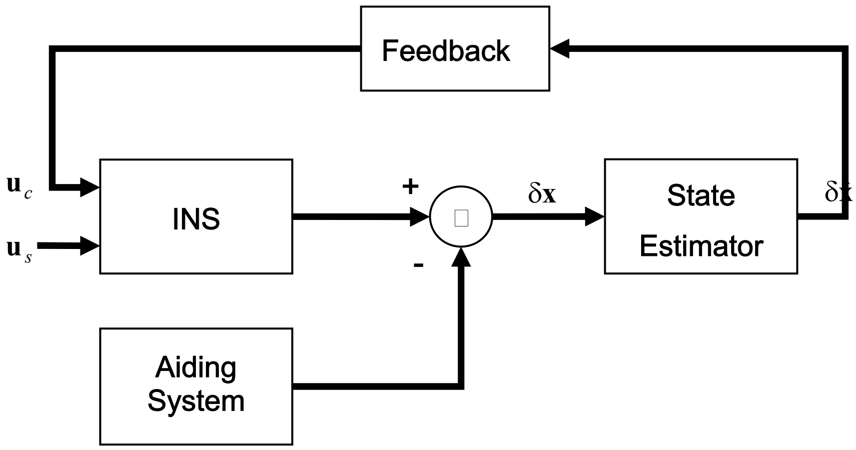

Figure 3-1 Aided Inertial Navigation System Representation

The observer may be our extended Kalman filter explained in CHAPTER 2. The input to the observer may not be the whole navigation states since some of the states may not be measurable or the external aiding source can not measure all navigation states. If our system is completely observable, feeding the observer even not with all of the system states will be adequate and the unmeasured states can also be estimated. In contrast to this, if the system is not observable, the navigation error states can not be estimated by the observer. This fact indeed, designates the success of the Kalman filter designed for the integration of INS and GPS.

INS error model derived in CHAPTER 2 and given by the equations 2.30 and 2.32, can be put into the form:

$$\delta\dot{\mathbf{x}} = \mathbf{A}(t)\delta\mathbf{x} + \mathbf{B}_s(t)\delta\mathbf{u}_s \tag{3.5}$$

where $\delta\mathbf{u}_s$ represents the sensor errors that are gyro and accelerometer biases for our case. The observer, Kalman filter, provides state error estimates to the system. A feedback loop can be generated and can be treated as the control input to the system. Then equation 3.5, attaching the observation equation, can be written in the form:

$$
\begin{aligned}
&\delta\dot{\mathbf{x}} = \mathbf{A}(t)\delta\mathbf{x} + \mathbf{B}_s(t)\delta\mathbf{u}_s + \delta\mathbf{u}_c \\
&\mathbf{y} = \mathbf{C}.\delta\mathbf{x} \\
&\delta\mathbf{u}_c = \delta\hat{\mathbf{x}}
\end{aligned}
\tag{3.6}
$$

In equation 3.6, $\delta\mathbf{u}_c$ represents the control/calibration input and $\delta\hat{\mathbf{x}}$ represents the Kalman filter state error estimates. Throughout these analyses, the sensor errors $\delta\mathbf{u}_s$, and control/calibration input $\delta\mathbf{u}_c$ will not be considered since they have no influence on the observability of the system.

Having defined the observability measure and constructed the aided INS representation, we can discuss the observability of our tightly coupled integration structure. For our case, both of the matrices are time varying, the $\mathbf{A}$ matrix has a constant size but size of the $\mathbf{C}$ matrix is not fixed. Number of satellites in view, i.e. number of measured pseudo and delta-range pair, changes time to time. This causes a change in the size of the $\mathbf{C}$ matrix. The number row of it may change from 2 to 24 (depends on the number of channels in the GPS receiver). Another case is that, the number of satellites in view may not be changing but the satellites that are used may be changing from time to time. For this case, the structure of the $\mathbf{C}$ matrix does not change but the values of its elements change so $\mathbf{C}$ matrix changes. Both of these cases change the observability of the system. As an intuitive consideration, the observability measure should increase as the number of satellites in view increases. Again intuitively, the change of satellites as the total number of them is fixed, should cause an immediate variation in the observability measure.

A more theoretical explanation is that if the number of the columns in the $\mathbf{C}$ matrix increases, the norm of $\mathbf{C}'(t)\mathbf{C}(t)$ product in $\mathbf{M}(t_0, t_f)$ increases so $\mathbf{M}(t_0, t_f)$ increases, inverse of $\mathbf{M}(t_0, t_f)$ decreases, inverse of norm of $\mathbf{M}(t_0, t_f)$ that is our observability measure increases. For the case that the number of satellites is fixed but the constellation changes, the norm of $\mathbf{C}'(t)\mathbf{C}(t)$ may increase or decrease depending on the values of the elements in the changing column. So observability measure may decrease or increase but surely it changes.

3.3.2 Computation of the Observability Measure

For our study, computation of the observability measure is done completely numerically in a finite time interval. A suitable integration step is chosen and at each integration step, the state transition matrix is calculated first. Then observability measure is found using this state transition matrix. As a last step, observability measure is calculated using equation 3.4.

Since our system is time varying, the state transition matrix $\mathbf{\Phi}$, and the observation matrix $\mathbf{C}$ change dynamically with time. $\mathbf{A}$ and $\mathbf{C}$ matrices are computed according to equations 2.30 and 2.32 in CHAPTER 2 respectively. But the computation of $\mathbf{\Phi}$ is done numerically by Euler Integration algorithm as

$$\mathbf{\Phi}(t_{k+1}, t_0) = \mathbf{\Phi}(t_k, t_0) + \mathbf{A}(t_k) \cdot \mathbf{\Phi}(t_k, t_0) \cdot \Delta t, \qquad \mathbf{\Phi}(t_0, t_0) = \mathbf{I}$$

Δt : Integration step

$t_k = k.\Delta t,$ and $k = 0,1,\ldots,\dfrac{t_f}{\Delta t}$

The observability Gramian given in equation 3.2 is also computed in discrete steps by Euler Integration algorithm as shown in the equation below.

$$\mathbf{M}(t_0, t_{k+1}) = \mathbf{M}(t_0, t_k) + \mathbf{\Phi}'(t_k, t_0) \cdot \mathbf{C}'(t_k) \cdot \mathbf{C}(t_k) \cdot \mathbf{\Phi}(t_k, t_0) \cdot \Delta t,$$
$$\mathbf{M}(t_0, t_0) = \mathbf{0}$$

As a last step, the observability measure is computed for each calculation step from t_o to t_f .using equation 3.4.

CHAPTER 4

EXPERIMENTAL RESULTS

4.1 Introduction

In this chapter, efforts to validate the designed integration architecture are given in detail. Experimental results are delivered to the reader in a way to compare the performance of the developed system to a reference system and as well as to a loosely coupled system.

4.2 Experimental Setup

All simulations are carried out offline but with real data. This in turn, leaded us to develop a system to collect data in real-time and then build an algorithm to process this data off-line. For this architecture, there exist problems in data synchronization between inertial measurement unit (IMU) and GPS data. To overcome this problem, a method is developed using the features of the current hardware setup. All these efforts are given briefly in this section dividing the situation into two sections as hardware and software organizations.

4.2.1 Hardware Setup

The hardware setup is composed of a vehicle, a special computer, a laptop computer, an inertial measurement unit, a GPS receiver and antenna, a reference navigation system and power supplies to feed these equipment.

A Land Rover jeep is the primary vehicle used for all testing. The tray in the rear houses the equipment used while data logging. Although a land vehicle, for which this thesis is developed, can maneuver under high speeds, our work is conducted at relatively low speeds not exceeding 50 km/h since, indeed the speed of the vehicle does not effect the performance of the system.

The IMU used in this thesis is a Northrop Grumman's LN-200 family of inertial equipment composed of 3 fiber optic gyros (FOGs) and 3 silicon accelerometers (SiAc's). It provides vehicle angular rate and linear acceleration. It satisfies tactical missile and guided projectile guidance requirements and aircraft flight control systems. It can be called low cost looking at whole grades of IMU's. A typical IMU of this grade exhibits several hundred kilometers of horizontal error in an INS run of 1 hour. Typical performance characteristics are given in Table 4-1 below. It is operated on RS-485 Serial Data Bus (SDLC). The sampling rate of the unit is 400 Hz and this rate is taken as the base for the navigation algorithm.

Table 4-1 Typical Characteristics of LN-200 IMU

Performance - Gyro	
Bias Repeatability	1deg./hr to 10deg./hr 1[sigma]
Random Walk	0.04 to 0.1deg.[sqr root]hr power spectral density (PSD) level
Scale Factor Stability	100 ppm 1[sigma]
Bias Variation	0.35deg./hr 1[sigma] with 100-second correlation time
Performance - Accelerometer	
Bias Repeatability	200 [micron]g to 1 milli-g, 1[sigma]
Scale Factor Stability	300 ppm 1sigma
Bias Variation	50 micro-g 1sigma with 60-second correlation time
White Noise	50 micro[sqr root]Hz PSD level

Figure 4-1 LN-200 Inertial Measurement Unit

The GPS receiver used in this thesis is an Ashtech G12 Sensor, a G12 GPS receiver enclosed in a box. It has 12 C/A code channels. It can output pseudo and delta-ranges what we call "raw data" at up to 10 Hz. It is operated on two independent standard RS-232 serial ports. But in normal operation, one of these serial ports is sufficient. It uses a standard L1 frequency antenna. The update rate that we use for raw data is 1 Hz and this is taken as the discrete Kalman filter measurement update frequency.

Figure 4-2 Ashtech G12 Receiver Board and G12 Sensor

The reference system used in this thesis is a Northrop Grumman's LN-100 family of inertial navigation system. It uses non-dithered Northrop Grumman Zero-Lock™ Laser Gyro (ZLG™) and A-4 accelerometer technologies together with a sophisticated tightly coupled Kalman filter that can give enhanced position, velocity, attitude, and pointing performance, as well as improved GPS acquisition and anti-jam capabilities. A grade of this inertial navigation system exhibits approximately 0.8 nautical miles in an INS-only run of 1 hour. It has an embedded

5 channel GPS receiver capable of delivering raw data. It is operated on a standard 1553B Data Bus.

Figure 4-3 Reference System – LN-100 Inertial Navigation System, Northrop Grumman

A single board computer (SBC) that is in a small form factor is used to read primarily IMU and also GPS time data. SBS has a card in one of its expansion slots that can read SDLC data. This card is used to read IMU data. A standard serial communication port on the SBC is also used to read GPS time data. The clocks used to operate the IMU are supplied by the timers embedded in this SBC.

GPS raw data is read by a separate laptop computer through a standard serial communication port. A second laptop is used to log the reference system's data. It has a PCMCI card to communicate on the 1553B Data Bus.

The utility is driven around ASELSAN's plant. Some part of this track is populated with trees, buildings, store tanks that cause GPS signal blockage. The test area and the track are shown in Figure 4-4 below.

Figure 4-4 Test Area and Track

4.2.2 Software Setup

There exists 4 distinct pieces of software:

- A real-time software running on the SBC to read and log IMU data and GPS time information.
- A Windows platform to read and log GPS raw data running on a laptop computer.
- A Windows platform to read and log reference system's data running on another laptop computer.
- Windows platforms to process the logged data on any separate PC.

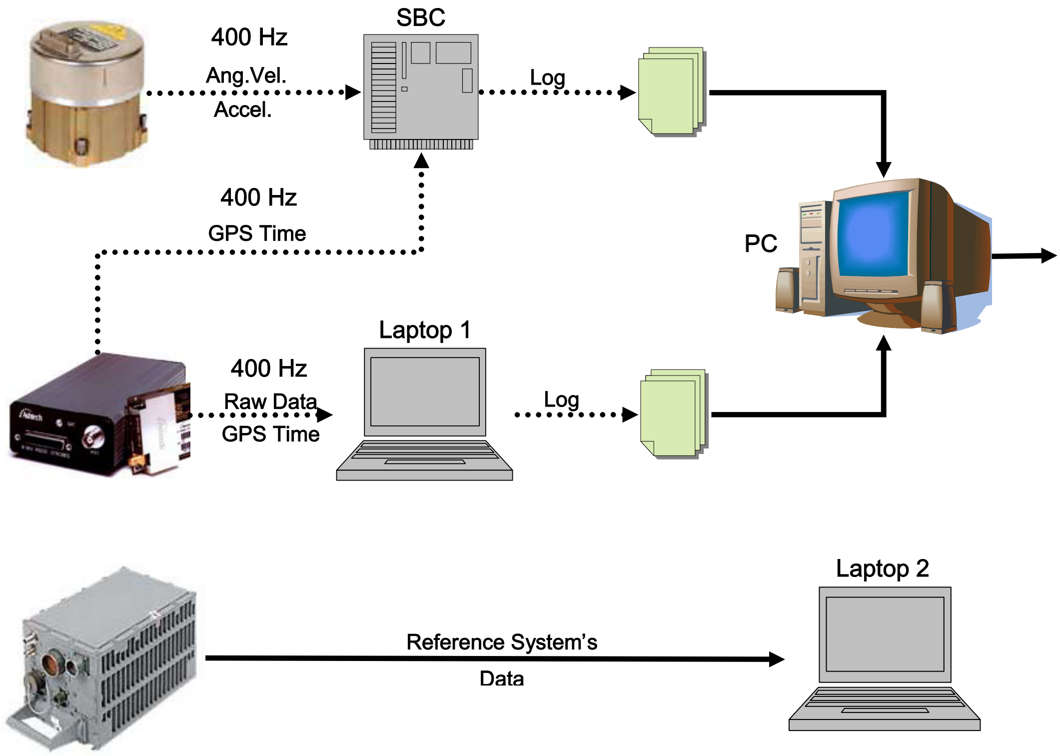

Figure 4-5 Hardware and Software Setup Summary

In SBC, IMU data is read in real time at 400Hz, which is the output rate of the IMU. On the other side, by the help of the serial port on the SBC, GPS time information is read from the first serial port of the GPS receiver. Time information obtained from GPS is sampled with 1 Hz frequency, so that each sample is repeated 400 times to reach the frequency of IMU. Corresponding to each IMU data sample, there exists a corresponding GPS time information but GPS data repeats itself 400 times until a new set of time data arrives at SBC. IMU turn rate and accelerometer outputs are logged to a file together with the corresponding GPS time information.

GPS raw data, GPS time information and also some other useful information are recorded to a file at 1 Hz using the second serial port on the GPS receiver. For this purpose Laptop 1 is used The two serial ports on the GPS receiver work synchronously so that both GPS time information on these two ports belong to the same time.

Logging GPS time at both of these platforms makes it possible to synchronize the IMU and GPS data that is very important for navigation applications. We have GPS and IMU information recorded in two separate files and logged GPS time at both files; this is the key point in correctly merging these two files. At the recorded file on SBC, the sample where GPS time changed value is found and this GPS time value is noted. The same GPS time sample is found in the file recorded by Laptop 1. The simulation data is assumed to start at this sample and the rest of the data recorded before this sample is discarded on both files. So, by the help of this process two set of data in two separate files are synchronized.

We have IMU data and GPS raw data on files. We move them to a PC where our algorithms are implemented and our simulations take place. The navigation algorithm and the Kalman filter are developed in MATLAB. A MATLAB script function reads IMU data file at 400 Hz and GPS raw data file at 1 Hz. With IMU data, navigation algorithm is run at 400 Hz. This navigation algorithm constitutes the INS output. A Kalman filter runs at 10 Hz to propagate the system model and covariances in time. Measurement update in the Kalman filter is realized at 1 Hz corresponding to the GPS measurement instants. The Kalman filter estimates of the system error states are fed back to the system after the measurement updates are done.

Solving the differential equations governing the inertial navigation system needs the knowledge of initial position, velocity and attitude values. Especially the initial value of the attitude angles should be entered fairly accurate. Otherwise the accelerometers mounted on the body cannot accurately resolve the readings into earth axis and this causes errors on all of the navigation outputs. There are ways to calculate the initial attitude inside the INS (called initial alignment) but since we have a reference system of enough accuracy, we get these angles from our reference system. The initial velocities are taken as zero because data recording starts while the test vehicle is stationary. The initial value of position is taken from the self solution of GPS receiver.

4.3 Observability Results

This section presents the results of the observability analysis that was mentioned in CHAPTER 3. The algorithm, which calculates the observability measure, is embedded inside the entire algorithm which produces the integrated output. The recorded real data is used to produce the results.

4.3.1 Effect of Aiding Level on Observability

This section establishes the results of observability measure for only pseudo-range aiding against pseudo-range plus delta-range aiding. The type of aiding measurement should have an effect on observability. We can treat pseudo and delta-range outputs of GPS receiver as independent measurements because they are calculated from different sources. But indeed, the error on these measurements may have some correlation because of the internal architecture of the GPS receiver.

The plot given in Figure 4-6 is the result for dependency of observability on the measurement type. The duration of the simulation is about 320 seconds and the solid line designates observability of pseudo and delta-range aiding whereas the dashed line designates pseudo-range aiding. From the figure, it is seen that observability measure M_o increases with time which is an expected result. The M_o of the pseudo and delta-range aiding is always greater than the M_o of the pseudo-range only aiding during the simulation time although two curves are not clearly distinguishable from the figure. But, before 120 seconds although small, a difference is obvious and can easily be seen in Figure 4-6.

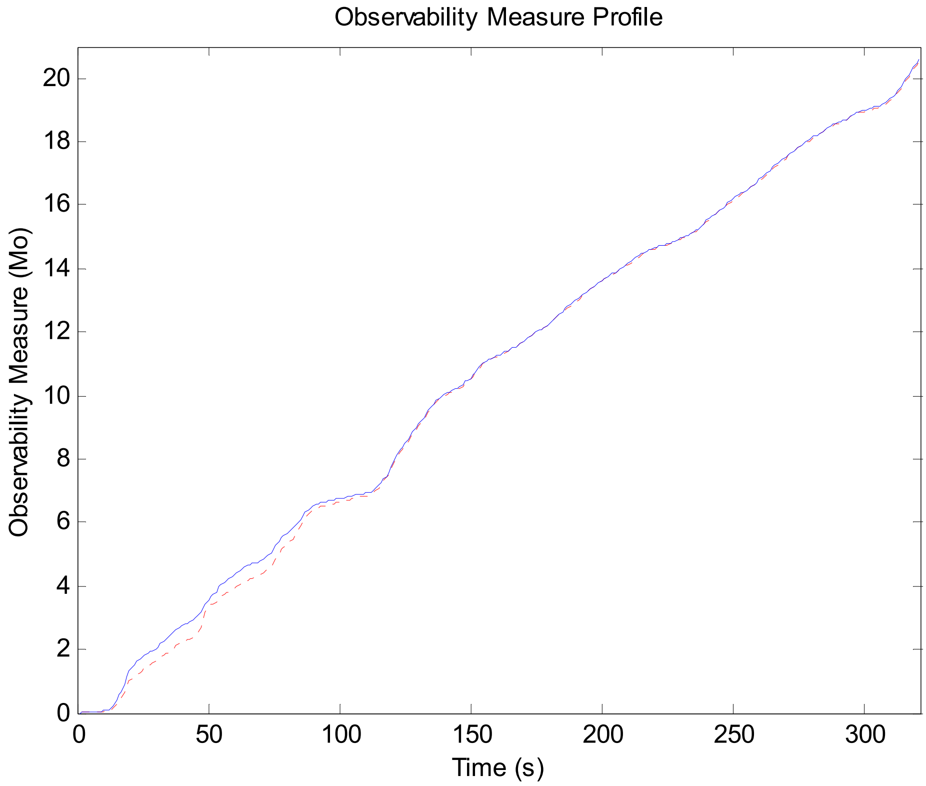

Figure 4-6 Observability measure for pseudo-range vs. pseudo and delta-range aided systems

In Figure 4-7, the time interval from 0 – 120 seconds is enlarged to see the details. Although the observability measures increase with time for both systems, their characteristics differ in this interval. After 120 seconds, M_o's of both systems get closer to each other and they behave similarly. It can be shown that the intervals where the rate of change of these curves increase correspond to time instants when the number of satellites in view increases. The opposite is also true; intervals where the rate of change of these curves decrease correspond to time instants when the number of satellites in view decreases. The observability measure is very small up to time 14. In that interval, the vehicle is stationary and then at time 14, the vehicle starts moving. At that instance, we see a sudden increase in M_o. This tells us that the motion and maneuvers of the vehicle increase observability. In fact, this result was discovered in other recent studies but here, we see it more obviously. To support this fact, we can show that at time 50, the vehicle makes a 90 degree turn and this causes a sudden change in M_o of especially the pseudo-range only aided system. Also we see that, reaction of the observability of the pseudo and delta-range aided system to the vehicle maneuvers is less. After time 120, the curves seem to be smoother. This means that as time increases, the change in number of satellites and vehicle maneuvers affect the observability measure less.

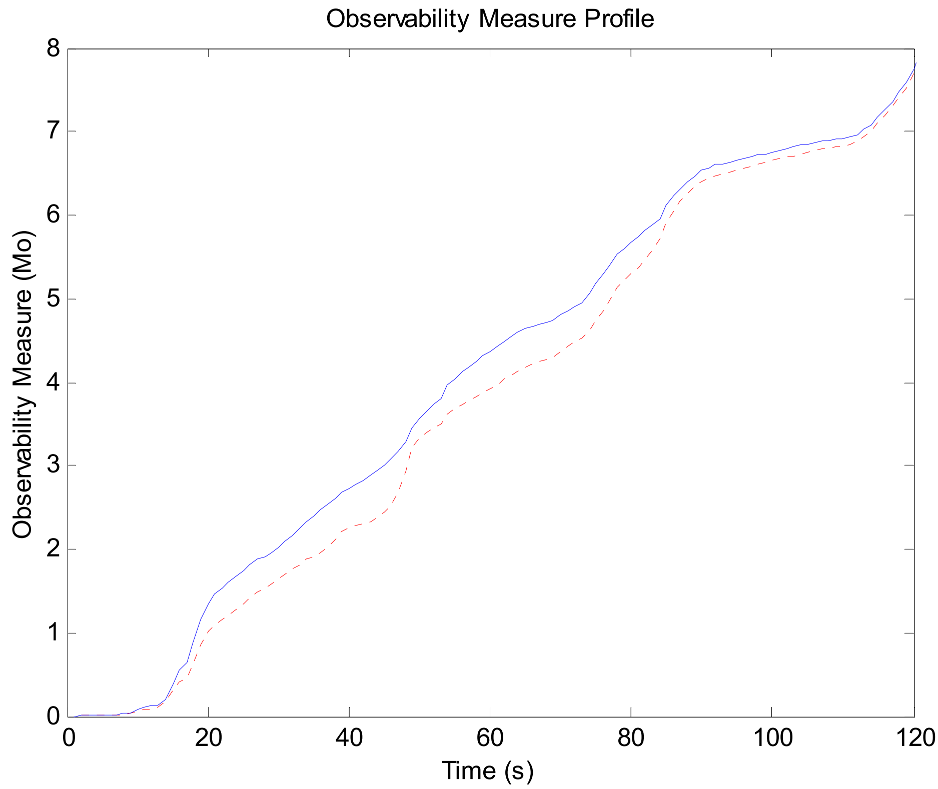

Figure 4-7 Enlarged view of 0-120 sec. interval

4.3.2 Effect of Number of Satellites on Observability

In CHAPTER 3, section 3.3.1, we stated that an increase in the number of pseudo and delta-range measurements, i.e. the number of visible satellites, should have a positive effect on the observability of the system. In order to prove this, the results of some simulations are presented in this section. The simulations are done with the same data used for the previous section. The results are shown for only pseudo and delta-range together aiding since the results of the two are very similar. To see the effect of number of satellites on observability, we made four simulations. In the first simulation, all of the satellites in view are used to calculate the observability measure of the system. In other simulations, the number of satellites used in the INS – GPS integration algorithm is decreased to 2 step by step starting from 4 satellites. So, totally 4 simulations are established. In each simulation, the satellites that are used may change during the simulation but the number of them is fixed. By doing so, we also wish to see the effect of satellite change on observability while the number of satellites are kept fixed.

In Figure 4-8, observability measures of simulations using all satellites, 4 satellites, 3 satellites, and 2 satellites are seen in the figure from top to bottom respectively. As an expected result, the observability of the system that uses all of the satellites in view is far more than the others. Also, the increase in the observability measure as the number of satellites increase is gathered from the figure. We see sudden changes in observability measures of 2 and 3 satellites cases. These jumps correspond to time instants that one (or more) of the satellites used in the simulations change. We can show the sudden increase at time 152 of the 2 satellite case and increase at time 38 of 3 satellite case as an example for this. We also observe that, all of the satellite changes do not cause sudden variations in the observability measure. Change of some satellites cause smoother increase or decrease in the rate of change of the observability measure. One other thing is that, as the number of satellites increase, the effect of satellite change becomes less effective.

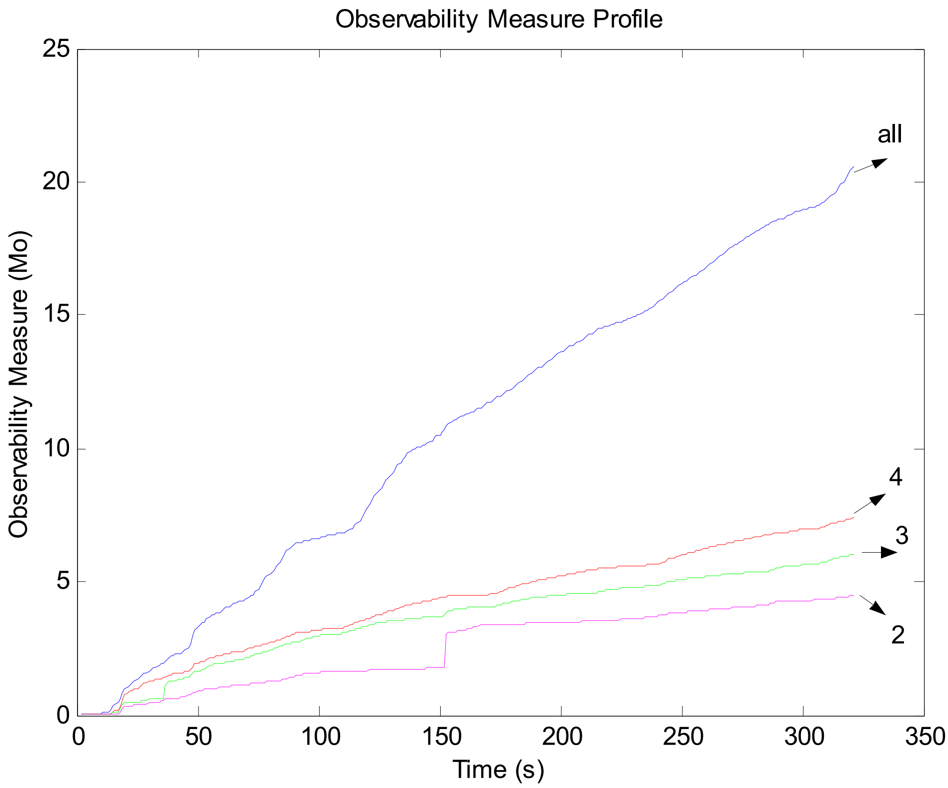

Figure 4-8 Result for the Effect of Number of Satellites on the Observability

4.3.3 Observability Measure Comparison with a Loosely Coupled System

In order to compare the observability measure of a tightly coupled system to a loosely coupled one, we made a simulation similar to previous ones but this time we used our real data to compute the observability measure of a loosely coupled system. This loosely coupled system is developed for the same sensors and use only GPS position measurement as an aiding. The result for the observability measure of this system is shown in Figure 4-9. We see that the observability measure M_o is very small (in the order of 10^{-3}) compared to the tightly coupled system. This is expected because the results which are presented in Koyaz (2003) for only position aiding is similar to our results. In the figure, observability measure increases with time and the huge increases in M_o correspond to time instants of vehicle's sharp maneuvers. For this system, to reach the M_o level of the tightly coupled system will probably take very long time.

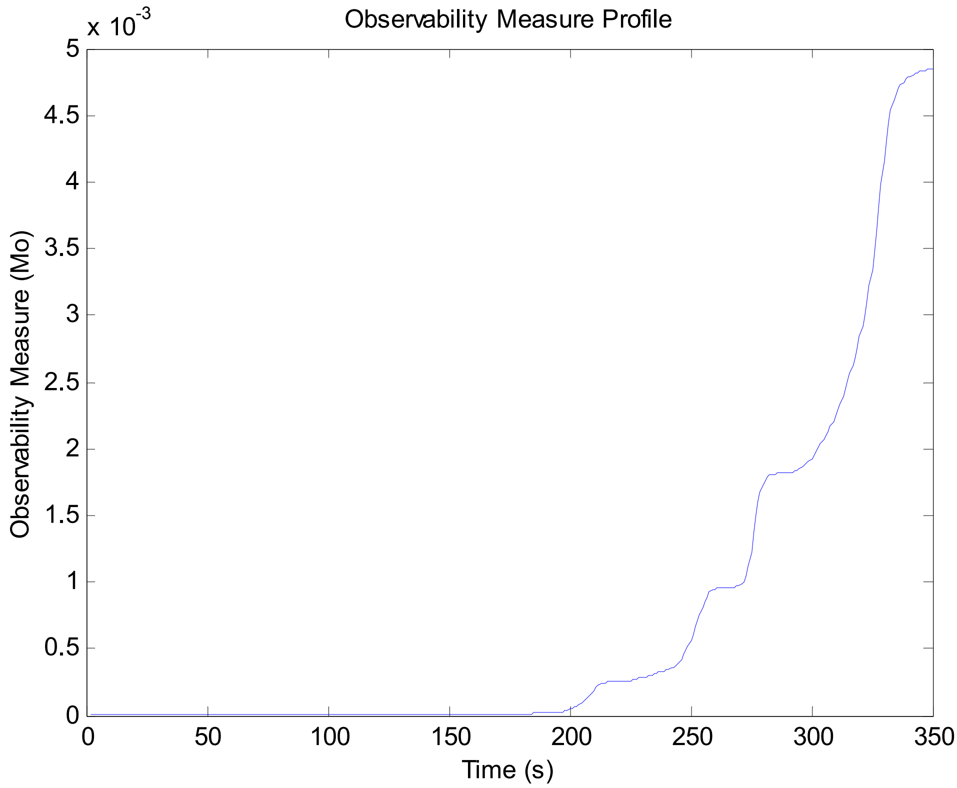

Figure 4-9 Observability Measure of the Loosely Coupled System

4.3.4 Discussion on the Results of Observability Analysis

Considering the simulation results and in the light of the theoretical knowledge, it is seen that:

- Tightly coupled integration structure has a high level of observability.
- Aiding level, i.e. using only pseudo-ranges or using pseudo and delta-ranges together change the observability level. But the difference in the observability measure of these two levels is apparent only at the initial time interval. This time depends on various aspects in the system and in

the environment. From this time on, the observability of the two systems show nearly the same characteristics.

- The number of satellites used changes the observability of the system. The increase in the number of satellites increases the observability. But addition of some satellites may have less or more effect on observability.
- The tightly coupled system is still observable even when the number of satellites falls below 4. But the level of observability decreases.
- The change in the satellite constellation as the number of satellites is fixed, causes a sudden change in observability. This may be an increase or a decrease depending on the satellite.
- The accelerations and the maneuvers of the vehicle increase the observability. As this acceleration and maneuvers become sharper, the increase in the observability becomes more noticeable.
- As time increases, the observability of the system increases and the effects of the situations given above become less effective.
- A loosely coupled system using only GPS position outputs as a measurement, has a very low level of observability compared to the tightly coupled system.

4.4 Tightly Coupled Integration Results

4.4.1 Performance Results

In this section, the results of the simulations which are done to evaluate the performance of the tightly coupled system are presented. The data sets used for these simulations are different from the sets used for the previous section, but all the test conditions are same for both of them.

The time of simulation is about 650 seconds but to show the results, only 350 seconds part of this data is used. In Figure 4-10 below, the vehicle position is given for ECEF *X* and *Y* axes, but the starting point is assumed as the origin and displacements in meters from this point are written on both axes. As illustrated in this figure, the path starts at point *0m X*, *0m Y* and goes to direction pointed with 1 and following the directions of the arrows, ends at the same point. In Figure 4-11, *X*, *Y*, and *Z* components of the real track position is plotted with respect to time. In Figure 4-12, number of satellites in view corresponding to this track is plotted with respect to time.

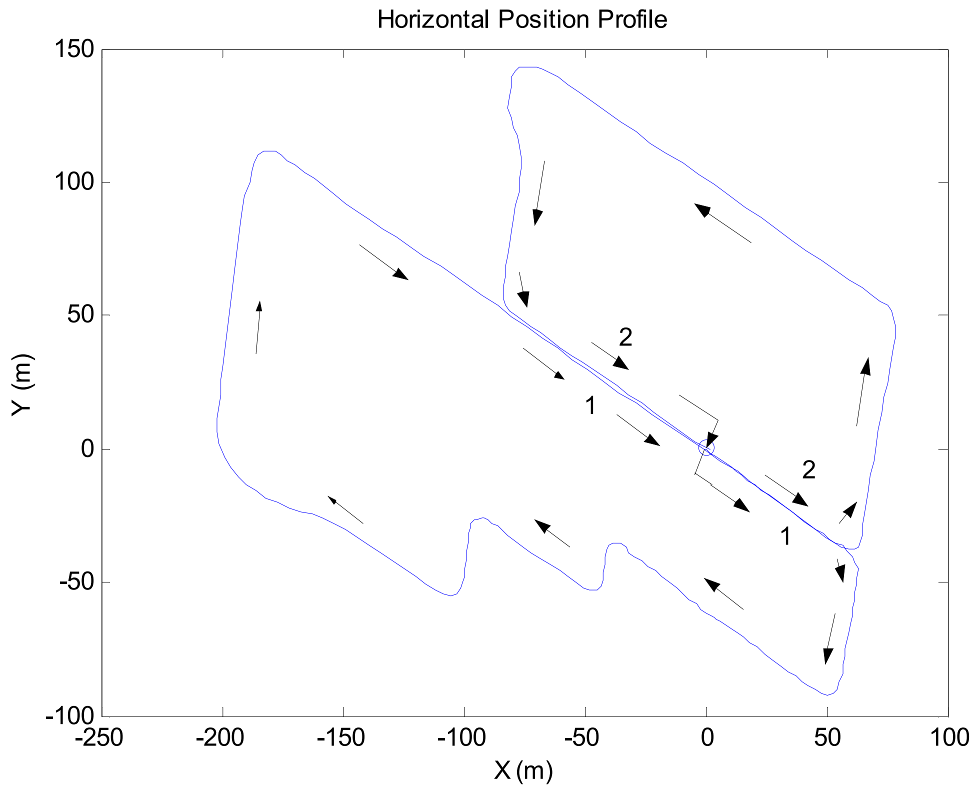

Figure 4-10 The Real Track and the Order of the Path

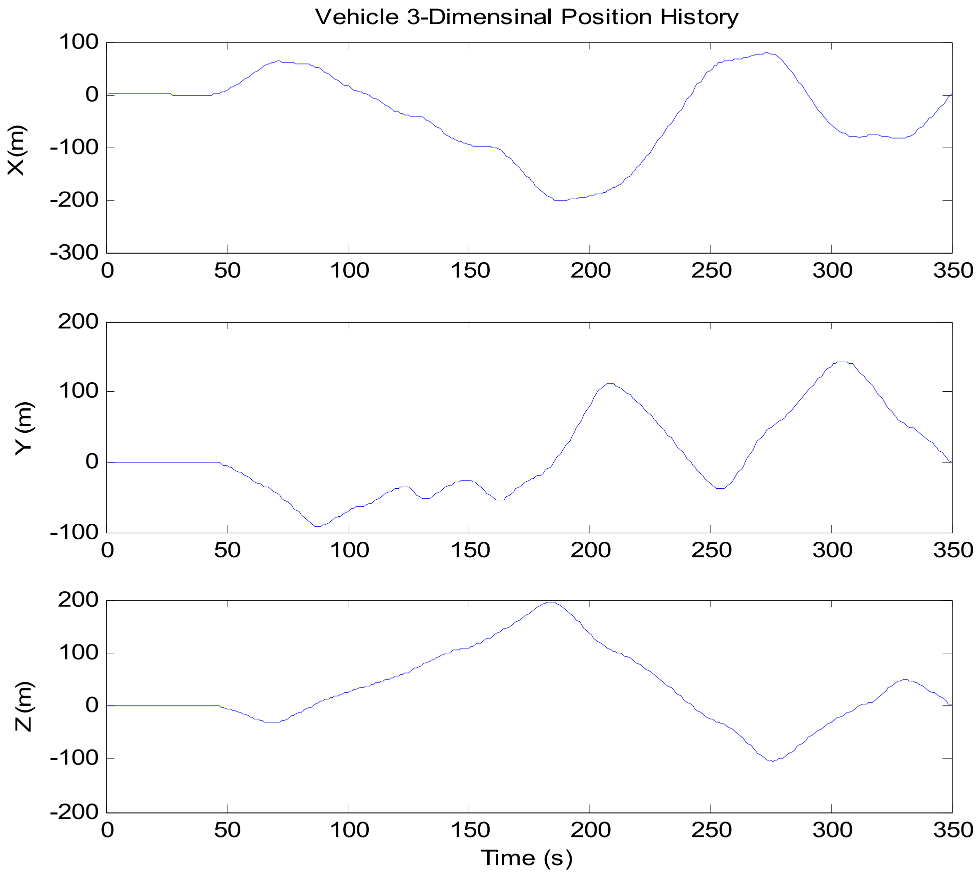

Figure 4-11 Vehicle 3-Dimensional Position Components with Respect to Time

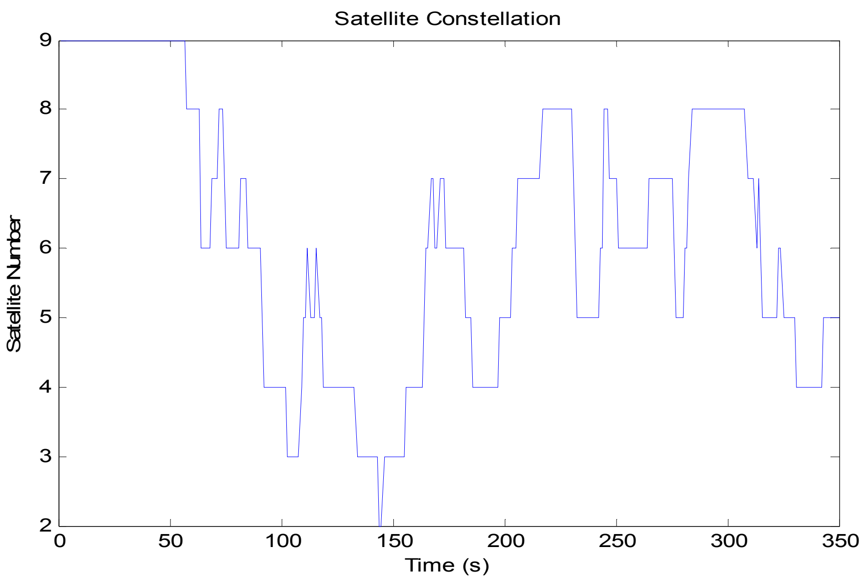

Figure 4-12 Satellite Constellation History Used in the Simulations

In Figure 4-13, the horizontal position of the vehicle is given for GPS-only and INS-only navigation solutions. The INS output is represented with a solid line whereas GPS output is represented with light colored crosses. As time increases the error in the INS-only solution increases and the track of INS goes far away from the real track, as expected. At time 350, INS position error is about 1150 meters. GPS solution seems better than the INS-only solution but it has gaps and sudden jumps in the position. A detailed view of the GPS position output can be seen in Figure 4-14. At the portion *-40 to -100m X* and *-40m Y*, a data gap of about 25 seconds occurs. Also we can see the high frequency faults occurred in the GPS output, for example at the portion *-70m*, and *80m Y*.

In Figure 4-15, the position output of GPS and tightly coupled system are given together. The fused output is represented with a solid line whereas GPS output is represented with light colored crosses. We see that the integrated system can successfully filter the GPS high and low frequency faults and can fill the data gaps of GPS.

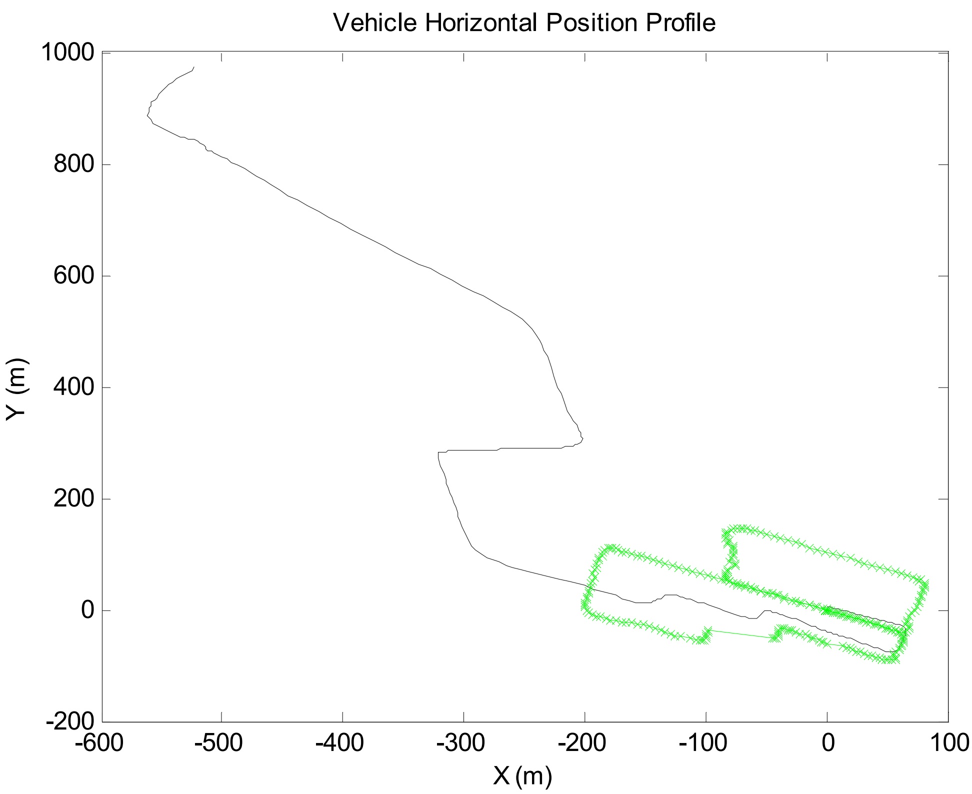

Figure 4-13 INS-Only and GPS-Only Position Outputs

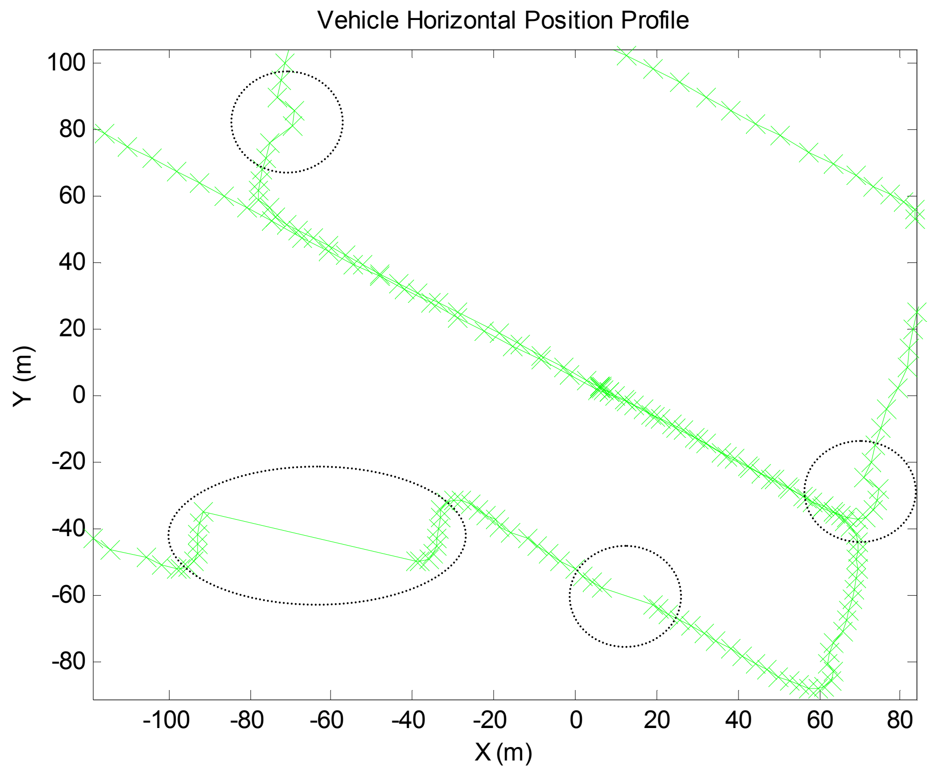

Figure 4-14 A Detailed View of the GPS Position Output

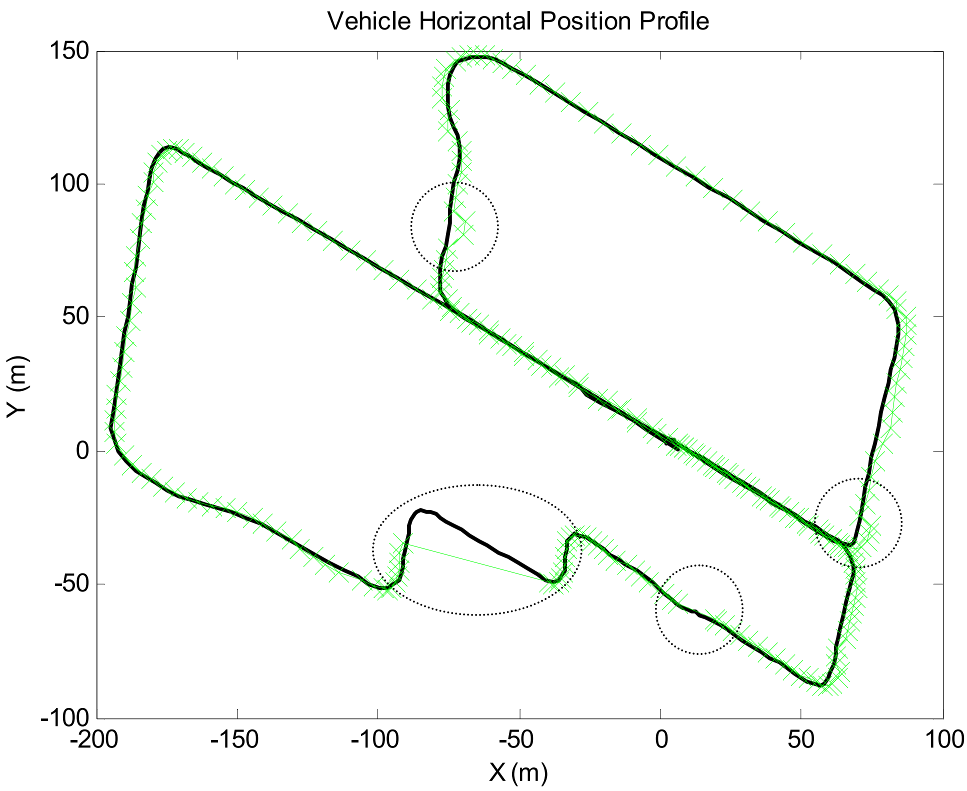

Figure 4-15 GPS and Tightly Coupled Integrated System's Outputs

In Figure 4-16, the position output of the reference system and the tightly coupled system are given together. The fused output is represented with a solid line whereas reference system's output is represented with light colored line. We see that the two outputs are very similar. At some portions, slight differences are observed. While evaluating these results, we should not forget that reference system does contain errors as well, but these comparisons certainly serve as a good starting point for confirming the performance of our integrated system.

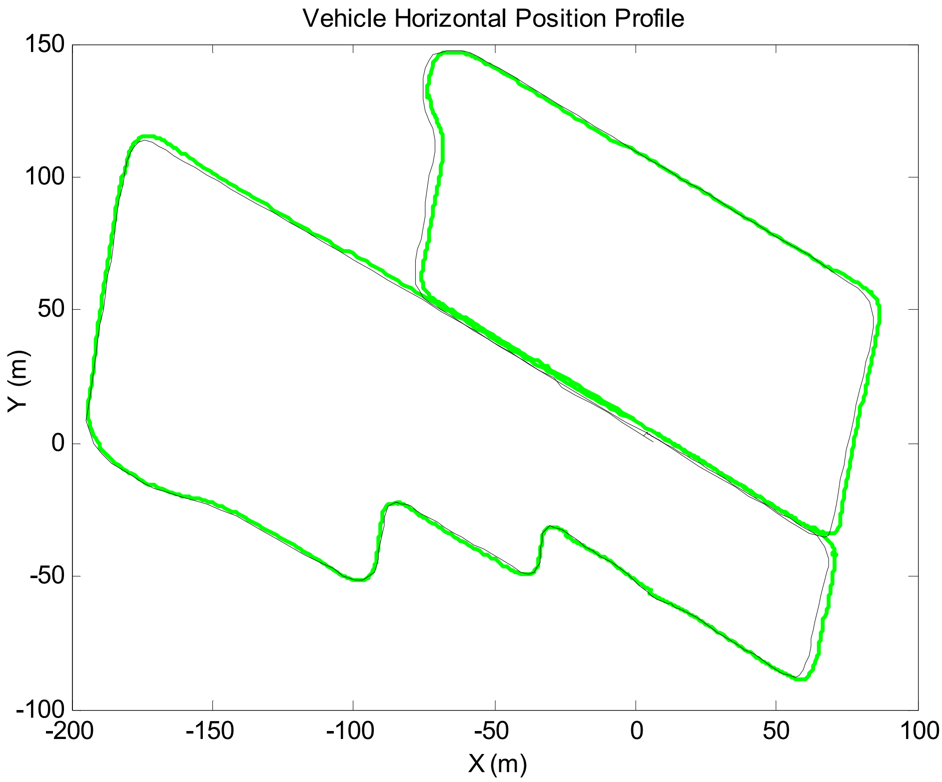

Figure 4-16 Reference System and Tightly Coupled System's Outputs

In Figure 4-17, errors in position output of our system with respect to the reference system are given together with the filter error covariance estimates. Error covariance estimates are represented with dashed – dotted lines. The errors in the 3 – dimensional position stay inside the bounds of the filter error covariance estimates for most of the time and this is an intended situation. The position error covariance goes down to a level under 2 meters. This performance is much better than the GPS position output which has a standard deviation of about 15 meters and INS output which has an exponential error growth characteristics with time. In Figure 4-18, and Figure 4-19, the filter error covariance estimates of velocity and attitude are presented respectively. The integrated system also bounds the errors in the velocity and attitude outputs. We see that, velocity error stays in the bound of 0.1 meters/second and attitude error stays in the bound of 0.25 degrees. The increases in the filter error covariance estimates of position and velocity that are seen in figures correspond to times that the number of satellites falls below 4. This result is consistent because at those times GPS measurements become week and INS outputs play more role in the filter output and filter informs this by increasing the error covariance.

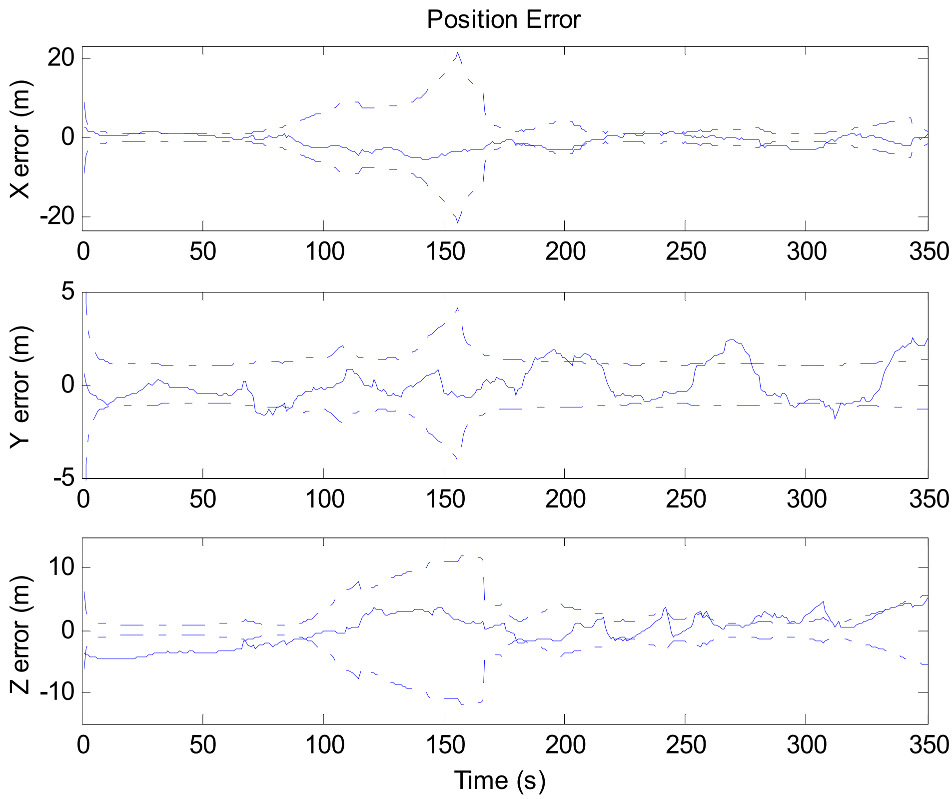

Figure 4-17 Position Error and Filter Position Error Covariance Estimates

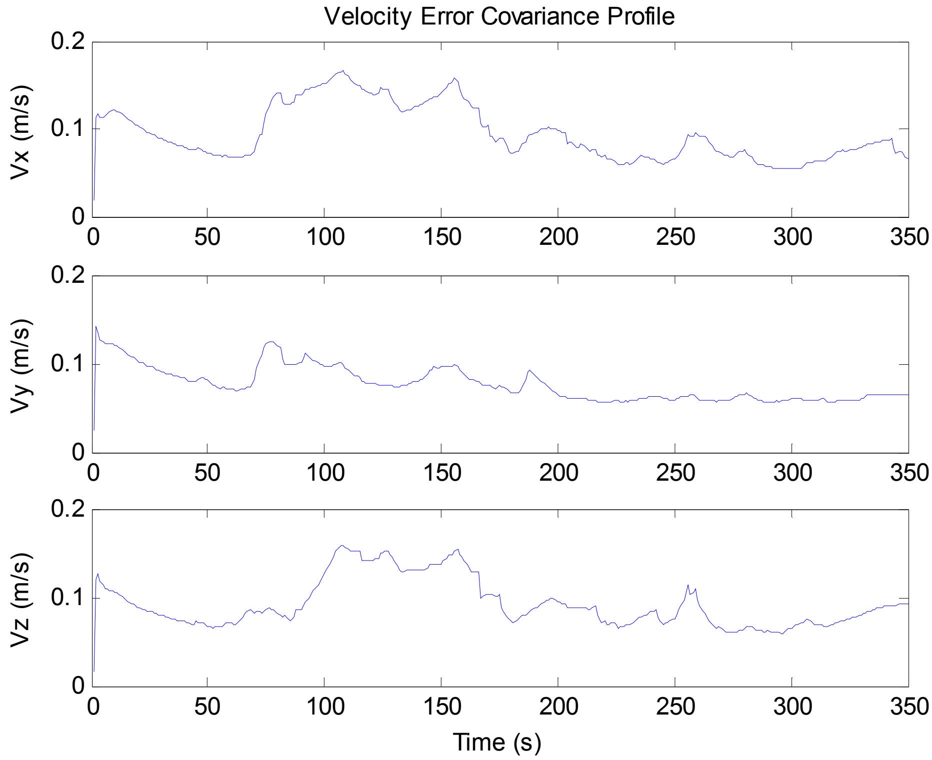

Figure 4-18 Filter Velocity Error Covariance Estimates

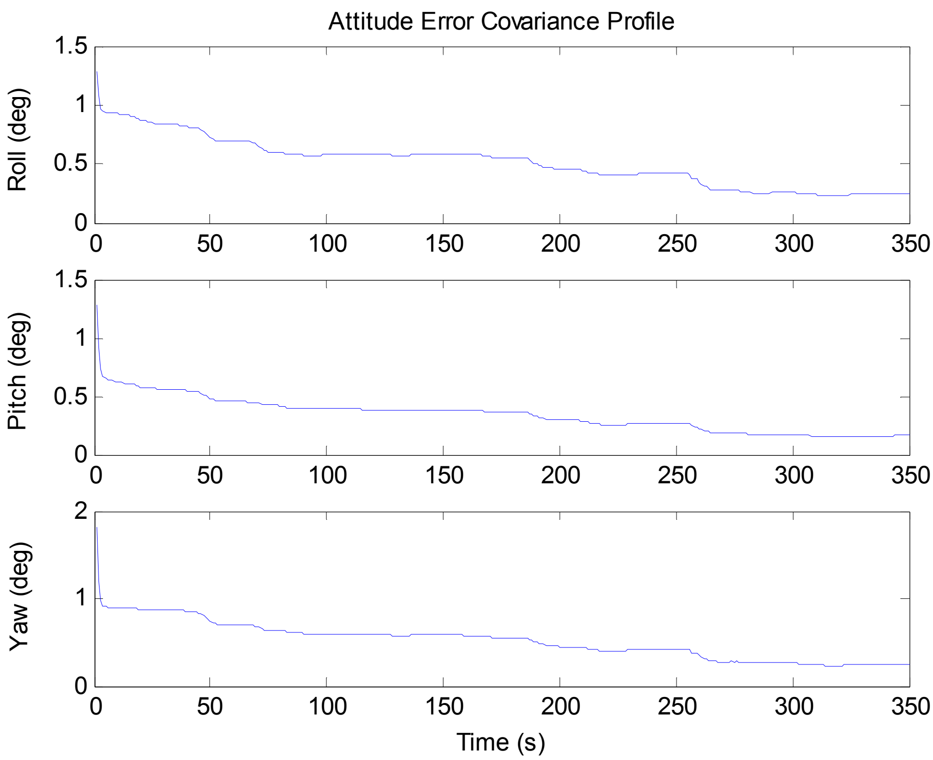

Figure 4-19 Filter Attitude Error Covariance Estimates

To simulate an environment where GPS signals are subject to serious blockage, we fed our system with less number of GPS measurements and presented the results in Figure 4-20, and Figure 4-21. In figures, solid line represents the integrated output and the light colored dashed line represents the real path. The time of simulation is about 250 seconds and first 60 seconds of this time is used for self – calibration of the system, i.e. all of the satellites are used to cancel the errors in the system. After time 60, which is marked with a circle on the path, the number of GPS satellites is decreased to 3 for Figure 4-20 and to 2 for Figure 4-21. We see that, even using only 3 satellites can give amazing performance. Integrated output follows the real track with a small error. Also for the 2 satellites case, the performance is adequate, but the error has more tendency to increase because, the errors in the INS starts to dominate the system. We can explain this result with the observability analysis that we made in the previous section. We have experienced that observability measure of the tightly coupled system with 3 satellites is smaller than the all satellites case but it is still high enough. The difference in the observability measures of scenarios carried out with different number of satellites, shows its effect in the performance of the position outputs as we can see from the results of the simulations in this section.

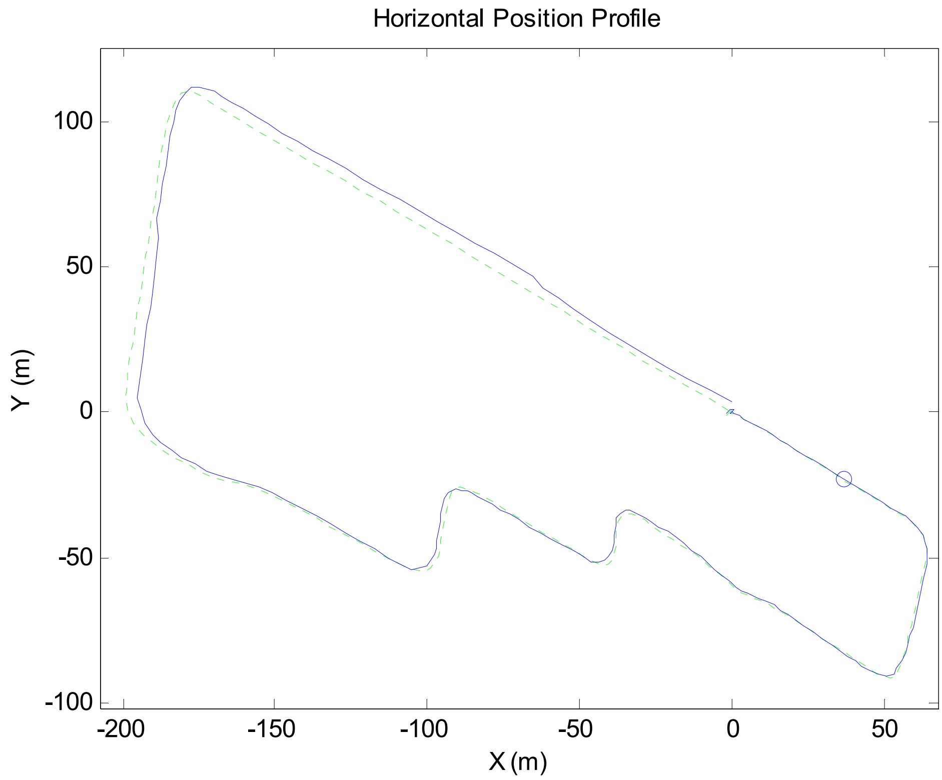

Figure 4-20 Integrated Position Output with 3 Satellites

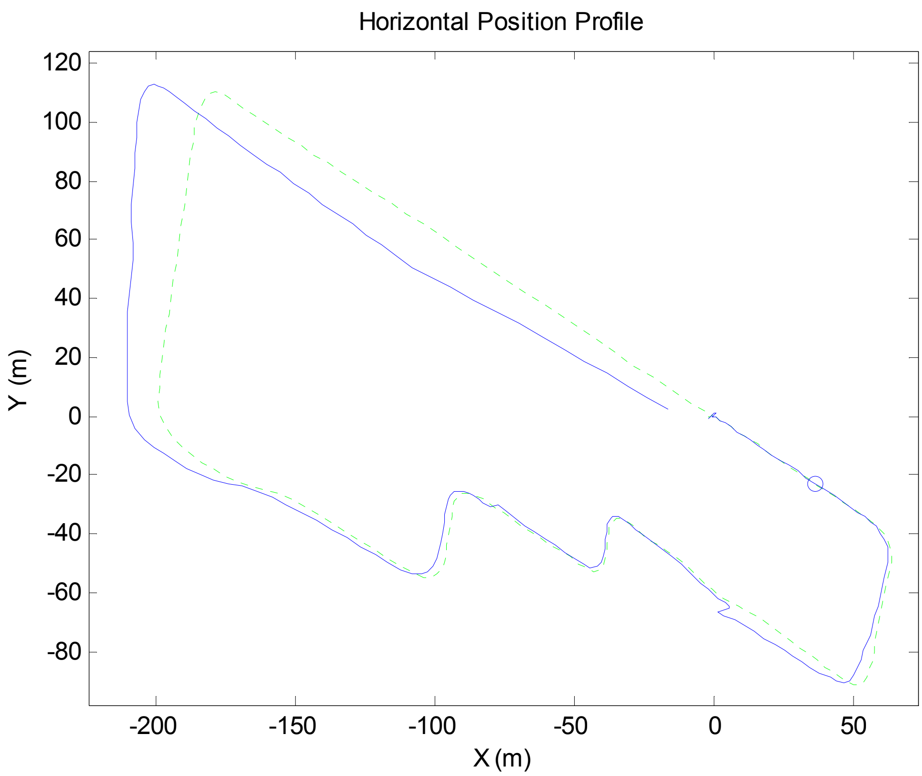

Figure 4-21 Integrated Position Output with 2Satellites

In CHAPTER 2, we have stated that the integrated system's ability to estimate sensor errors is an essential condition for self – calibration of the system. In order to show the effectiveness of the tightly coupled system in estimating the sensor errors, we present results of some simulations here. For the reason that, it is hard to know the real values of random gyro and accelerometer biases in an IMU, we injected external known biases to sensor readings and tried to estimate what we have injected. The extra biases are $2.5e^{-4}$ radians/second for gyros and 0.25 meters/second^2 for accelerometers. These biases are chosen to be 10 times the maximum expected biases in our IMU because what we read at the end will be the sum of the real IMU bias plus the extra bias. If real biases are small enough with respect to the extra biases, we should observe approximately the extra biases as the estimates of the IMU errors. In Figure 4-22, and Figure 4-23, the filter estimates of the gyro and accelerometer biases are presented. We see that, the convergence of the estimates to real values is fast except the Z gyro. In general, estimating the gyro bias in Z direction is difficult (Titterton (1997)), so the result is consistent. The estimation of biases in the X and Y gyro starts immediately and converges to a reasonable level by the time 50. That is really fast because the vehicle is stationary up to time 55. So we can conclude that the motion of the vehicle has less effect on the estimation of the gyro biases. For the biases in X and Y accelerometer, estimation begins by the time vehicle starts moving and they converge to reasonable levels immediately. So we can conclude that the motion i.e. the accelerations of the vehicle help the filter in estimating the accelerometer biases. For the accelerometer in the Z axis, the estimation starts immediately because there is already acceleration in that axis due to gravity that makes life easy.

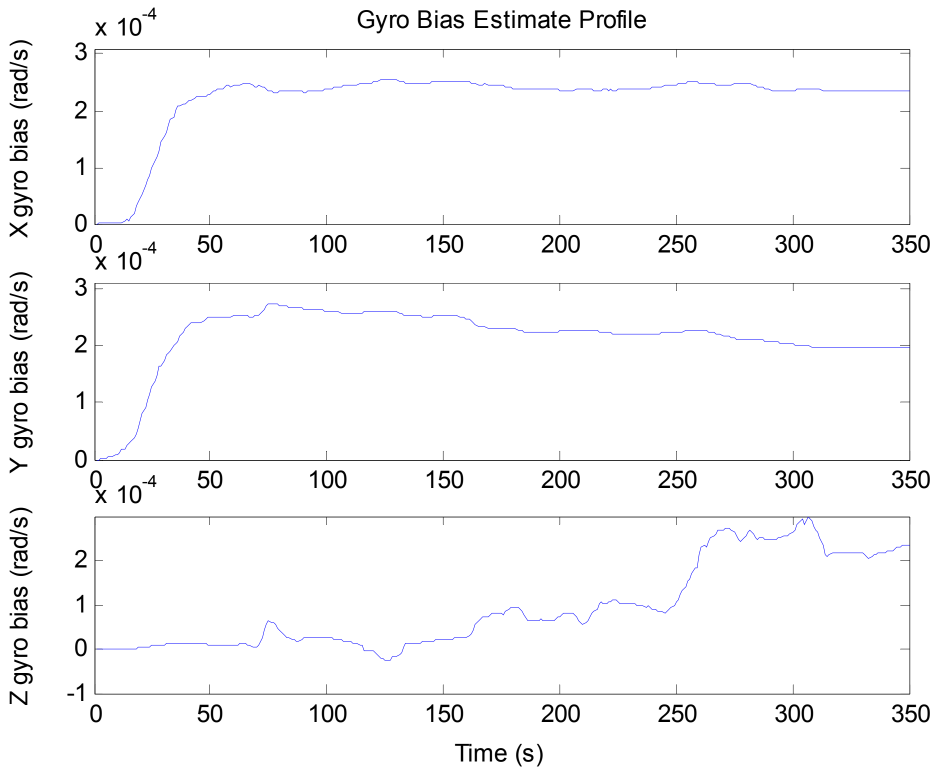

Figure 4-22 Gyro Bias Estimates of the Filter

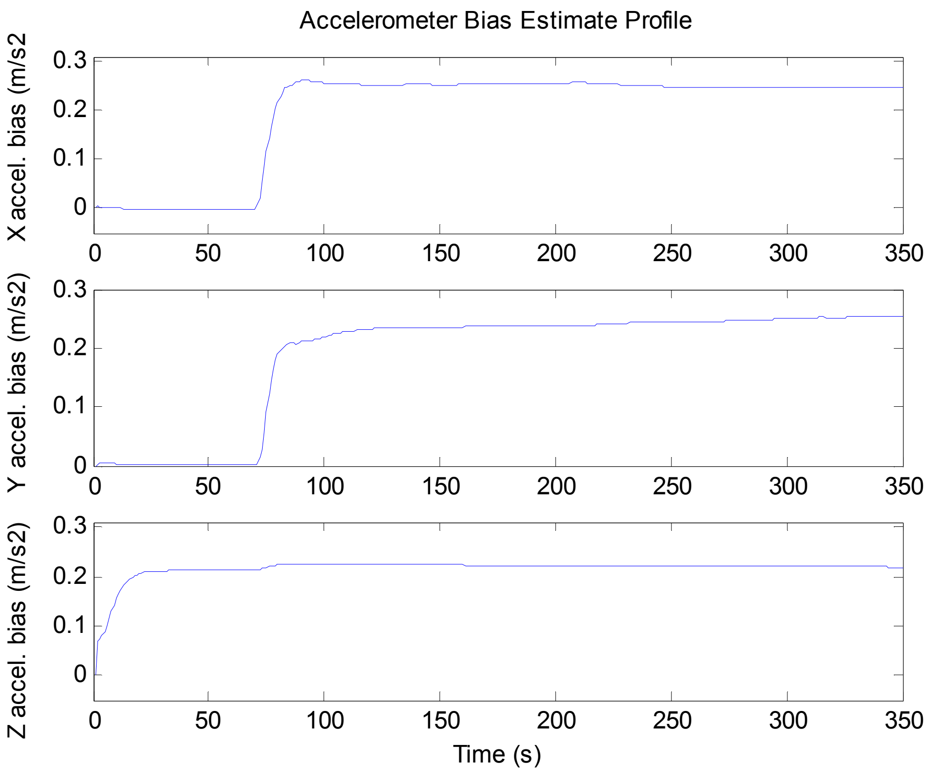

Figure 4-23 Accelerometer Bias Estimates of the Filter

4.4.2 Tightly Coupled and Loosely Coupled Integration Comparison

In this section, a loosely coupled system that was developed for the same sensors is used for comparison. The input data to the tightly and loosely coupled systems are the same and it is the data that is used for the previous section.

In Figure 4-24 below, horizontal position outputs of tightly coupled and loosely coupled systems are given together. The solid line represents the tightly coupled system and the line with crosses represents the loosely coupled system. For the parts of the track that the number of satellites is 4 or above 4, i.e. GPS produces position measurements, two curves are similar. Two circles marked on the figure point out the interval that no GPS position output is produced. In this 25 seconds interval, loosely coupled system's output swerves from the real track as seen in the figure.

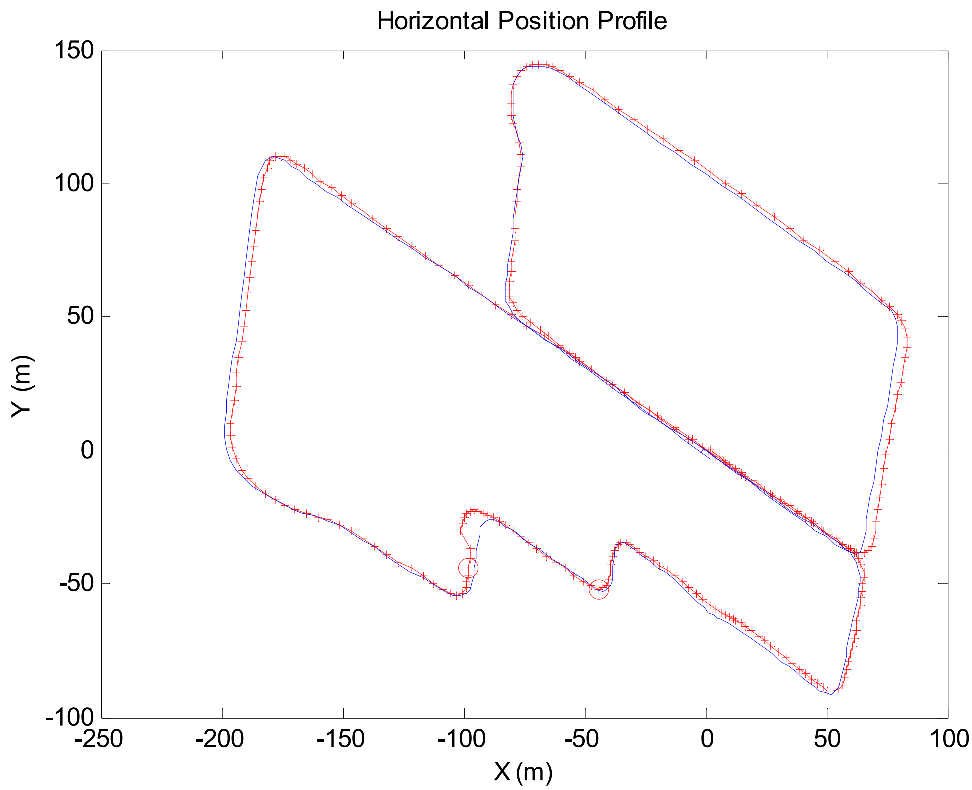

Figure 4-24 Tightly Coupled and Loosely Coupled Systems' Horizontal Position Outputs

To compare the performance of the two systems and to better see the difference, we have developed a scenario. In this scenario, a simulation of 350 seconds is done in the following manner:

- From the beginning to 60 seconds, we let both systems calibrate themselves, so we did not change the satellite constellation.
- For the next 60 seconds, we decreased the number of satellites below 4 so that GPS cannot produce position measurements but there are still pseudo and delta-range measurements available.
- For the next 15 seconds, we brought the satellites back into their original constellation and let the systems calibrate themselves.
- The scenario goes on like this with 60 seconds interruption and then 15 seconds normal operations until time 350.

The satellite constellation resulting from this scenario is shown in Figure 4-25 below.

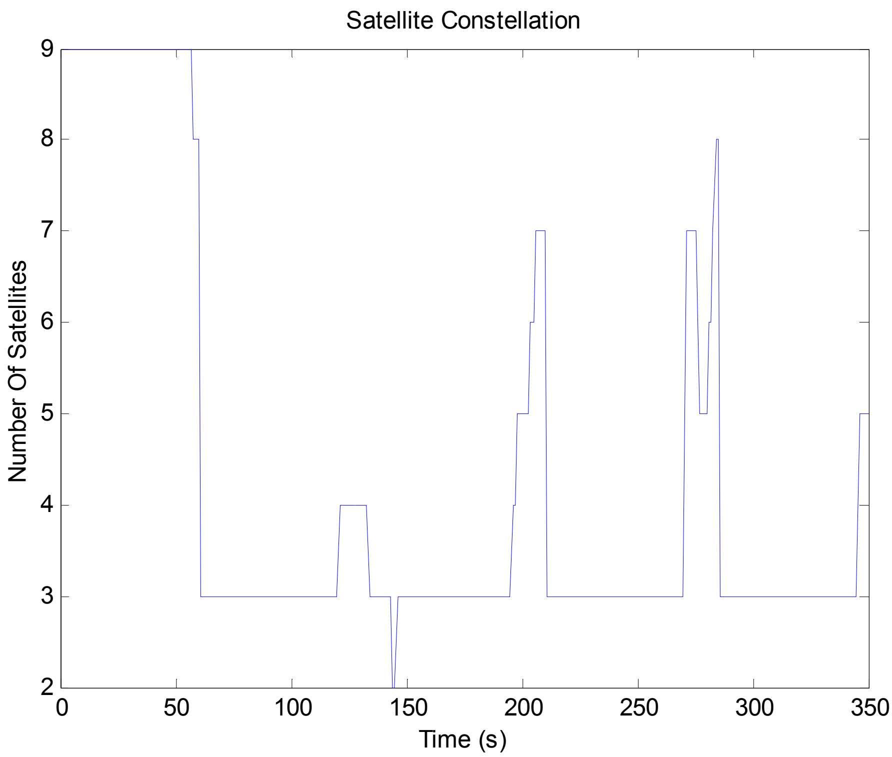

Figure 4-25 Satellite Constellation Summary Used in this Scenario

In Figure 4-26, the horizontal position outputs for the reference system, tightly coupled system and loosely coupled system are presented together. The reference system is represented with a dashed line, the tightly coupled system with circles and the loosely coupled system with crosses. We can see from the figure that the loosely coupled system cannot follow the true track when GPS position solutions are not available whereas tightly coupled system follows the track for most of the time. To summarize the result of this scenario and to better see the difference between two systems, we present the error – time plot of them with respect to reference system in Figure 4-27. In this figure, the horizontal position error in the loosely coupled system is represented with a dashed line and error in the tightly coupled system with a solid line. We observe that the error in the tightly coupled system is below 5 meters for most of the time while the error in the loosely coupled system is above 5 meters for most of the time. The errors in both systems have a tendency to increase with time but this tendency is more in the loosely coupled system. Since the observability of the loosely coupled system is less, 15 seconds of measurement time is not sufficient to estimate and correct the errors in the system. The tightly coupled system makes use of its high level of observability and can estimate and correct the errors in the system in an interval of 15 seconds.

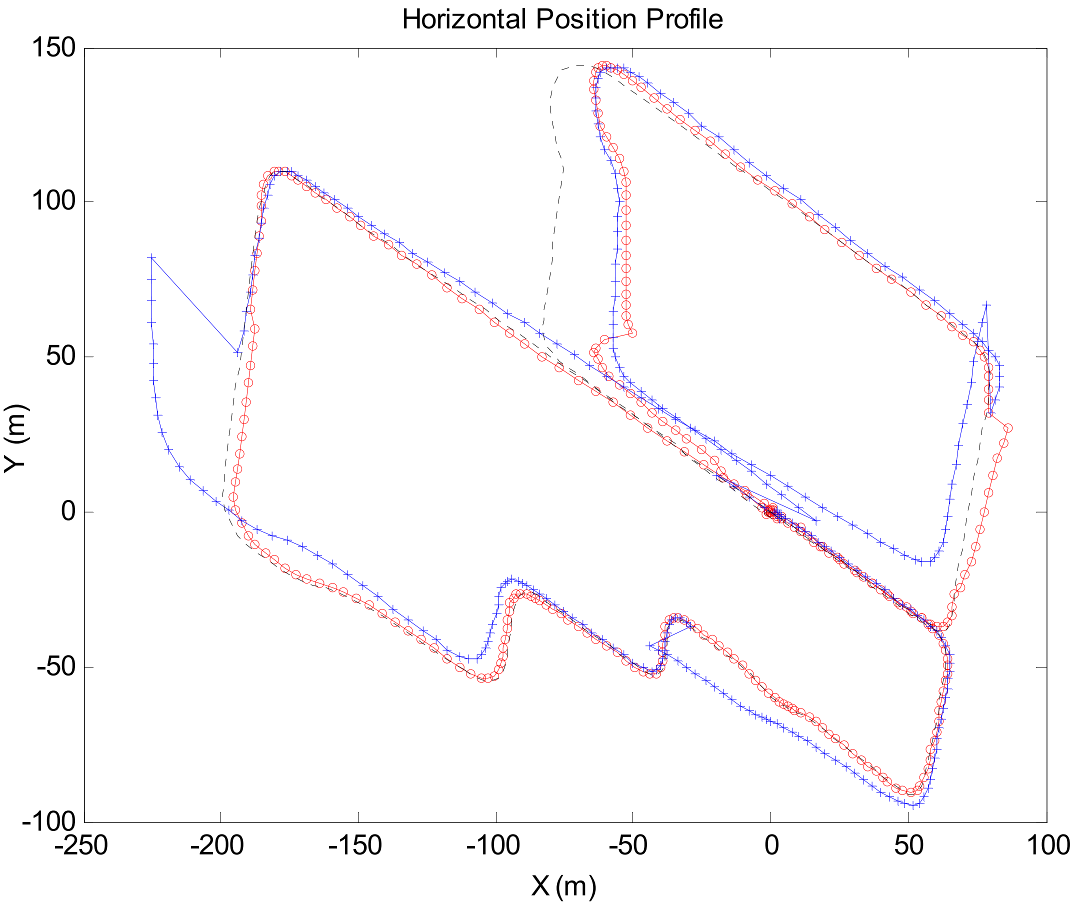

Figure 4-26 Horizontal Position Output for the Reference System, Tightly Coupled and Loosely Coupled Systems

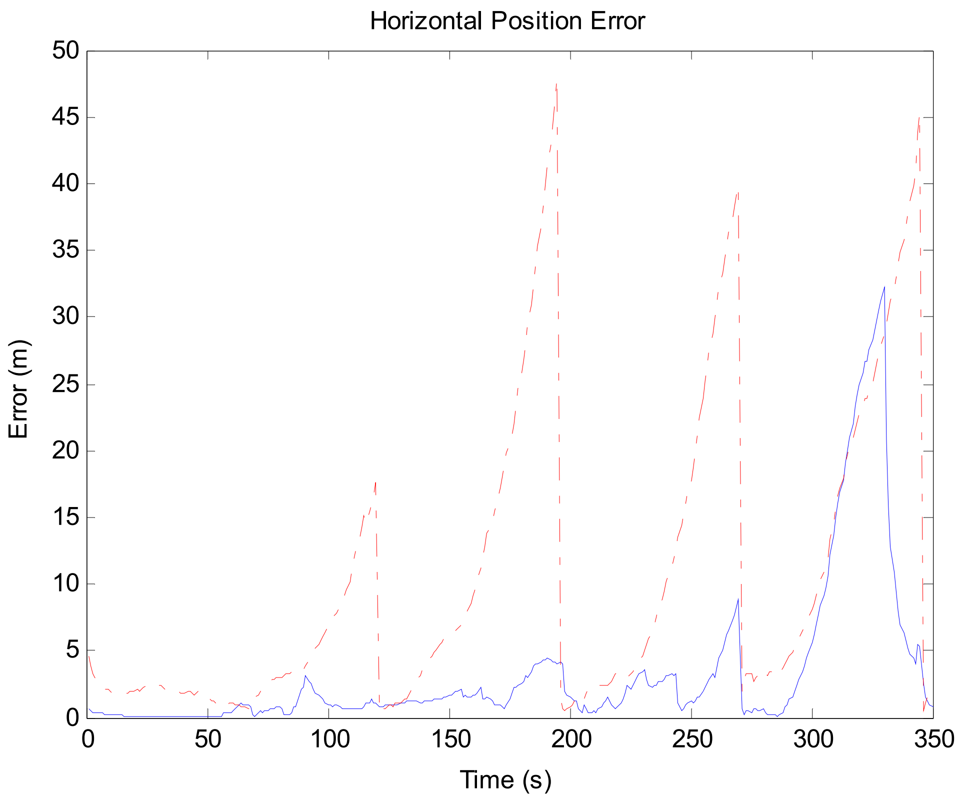

Figure 4-27 Horizontal Position Errors for Tightly and Loosely Coupled Systems

4.4.3 Discussion on the Results of Tightly Coupled Integration

In this section, we presented the general performance of the developed tightly coupled integration architecture comparing it to a reference system and also to a loosely coupled system. In the light of simulations we can conclude that:

- The designed tightly coupled Inertial/GPS navigation system provides accurate position velocity and attitude information.
- It corrects the time dependant errors in the INS and high frequency errors in the GPS and provides superior performance compared to both.
- The tightly coupled architecture decreases the dependency on GPS navigation solutions which is a problem in the loosely coupled architecture.

- The developed system provides accurate navigation solutions even when the durations that the number of satellites below 4 are long.

- The system can effectively estimate and correct the sensor errors, gyro and accelerometer biases.

- The system has a superior performance compared to a loosely coupled system on both aspects of observability and the accuracy of the navigation solutions.

CHAPTER 5

CONTRIBUTIONS, CONCLUSIONS AND FUTURE WORK

The contribution of this study is the assessment of the performance of a tactical-grade IMU integrated with a standard GPS receiver for high-accuracy navigation. In this regard, a comparison of two integration strategies is also performed to assess their relative performance. In particular, loosely coupled integration, and tightly coupled integration strategies are considered. Some new hardware and software is also developed as part of this work and were used to prepare the results which are presented in the previous chapter.

The performance parameters used to assess the above system included position accuracy during complete and partial GPS data outages, observability of the system both in normal and adverse conditions, as well as the overall accuracy of the system.

Determination of the accuracy level which can be achieved through a tightly coupled integration strategy using the sensors in hand is a great benefit on its own. In addition to this, seeing the limitations in accuracy that is caused by some system parameters is also important.

The observability analysis made in this study for the tightly coupled integrated navigation system and comparison of the results with a loosely coupled system has never been touched on before in the literature. The quantitative and qualitative results obtained from this analysis and comparing them with the intuitive a priory information about observability is also another contribution.

Details of the major conclusions of this study are summarized below in terms of the objectives set out in CHAPTER 1.

Integrated System's Reliability

- The integrated system shows better performance than GPS-only and INS-only in all cases.
- The integrated system can successfully estimate the inertial sensor errors in INS.
- The integrated system can successfully filter the high frequency faults and can accurately fill data gaps in GPS.

System Positioning Accuracy During GPS Data Outages

- For all simulated data outages, the tightly coupled integration strategy outperformed the loosely coupled integration strategy.
- The loosely coupled system cannot provide accurate results for data outages longer than 20 seconds.
- For complete data outages of long durations, the tightly coupled integrated system can provide accurate results with only 3 satellites. For 2 satellites, this duration decreases by a small amount.
- For discontinuous GPS data simulations, the tightly coupled system has higher power of estimation for longer durations compared to the loosely coupled system.

Observability of Aided Navigation System

- Delta-range measurement does not have significant effect in the system observability for long simulation times.

- For the tightly coupled integration, the observability of the system increases with an increase in number of satellites.

- The tightly coupled system remains observable even when number of satellites is less than 4.

- The observability of the tightly coupled system is much greater than the loosely coupled system.

Impact of Integration Strategy On Overall System Performance

- The tightly coupled integration strategy outperformed the loosely coupled integration approach, although in some circumstances these differences were not significant.

- The tightly coupled system removes the dependency on GPS navigation solutions.

- The tightly coupled system can reduce the filter error covariance estimates to a lower level compared to the loosely coupled system.

There are many avenues that can be progressed from this thesis. The observability analysis made in this study examined the overall observability of a time varying system. The analysis can be expanded to studies concerning the observability of individual states of the system. This approach may help in deeper understanding of the nature of aided INS, so improvements in performance of some outputs can be obtained. Another useful field will be the implementation of fault detection algorithms to increase the integrity of the system. In this study, measurements from the GPS are directly used which can cause misoperation in a jamming environment. Addition of self-detection algorithm which can check integrity of pseudo and delta-range measurements are inevitable for military and critical civilian applications of integrated navigation systems.

REFERENCES

[1] Akçayır, İ., "Aided Land Navigation System", M.S. Thesis, Hacettepe University, Department of Electrical and Electronics Engineering, 2003.

[2] Biezad, D.J., "Integrated Navigation and Guidance Systems", AIAA Inc., VA, 1999.

[3] Britting, K.R., "Inertial Navigation System Analysis", John Wiley and Sons, Inc., 1971.

[4] Brockett, R.W., "Finite Dimensional Linear Systems", John Wiley and Sons, Inc., 1970.

[5] Chatfield, A.B., "Fundamentals of High Accuracy Inertial Navigation", AIAA Inc., 1997.

[6] Daljit, S and Grewal, H., "Autonomous Vehicle Using WADGPS", Proceedings of the ION GPS-95, September 12-15, Palm Springs, California, pp-1333-1338, 1995.

[7] Gelb, A., "Applied Optimal Estimation", The M.I.T. Press, 1974.

[8] Greenspan, R. L., "GPS and Inertial Integration", B. Parkinson and J. J. Spilker, Jr., eds., Global Positioning System: Theory And Applications, volume 2, chapter 7. American Institute of Aeronautics and Astronautics, Inc., 1996.

[9] Grewal M.S., Weill L.R., "Global Positioning Systems, Inertial Navigation, and Integration", John Wiley and Sons, Inc., 2001.

[10] Hartman, R. G., "An Integrated GPS/IRS Design Approach", Navigation Journal of the Institute of Navigation, 35(1), pp.121-134, 1988.

[11] ICD-GPS-200C, “Navstar GPS Space Segment / Navigation User Interfaces Revision C”, GPS NAVSTAR JPO, 2000.

[12] Jekeli, C., “Inertial Navigation Systems with Geodetic Applications”, Walter de Gruyter, 2000.

[13] Koyaz, P., “A System Theoretical Approach to Inertial Navigation”, Ph.D. Thesis, Middle East Technical University, Department of Electrical and Electronics Engineering, 2003.

[14] Meskin, D.G., and Bar-Itzhack, I.Y., “Observability Analysis of Piece-Wise Constant Systems- Part II: Application to Inertial Navigation In Flight Alignment”, IEEE Trans. on Aerospace and Electronics Systems, vol.28, no.4, October 1992, pp.1068-1075.

[15] Ohlmeyer, E.J., Pepitone, T.R., and Miller, B.L., “Assessment of Integrated GPS/INS for the EX-171 Extended Range Guided Munition”, AIAA Guidance, Navigation, and Guidance Control Conference, 1998.

[16] Regan, F.J., “Strapdown Systems, Part II, Algorithms”, Naval Surface Warfare Center, 1981.

[17] Rogers, R.M., “Applied Mathematics in Integrated Navigation Systems”, AIAA Inc., 2000.

[18] Salychev, O., “Inertial Systems in Navigation and Geophysics”, Bauman MSTU Press, 1998.

[19] Sukkarieh, S., “Low Cost, High Integrity, Aided Inertial Navigation Systems for Autonomous Land Vehicles”, Ph.D. Thesis, University of Sydney, Department of Mechanical And Mechatronics Engineering, 2000.

[20] Titterton, D.H., and Weston, J.L., “Strapdown Inertial Navigation Technology”, Peter Peregrinus Ltd., London, 1997.